

Abbreviations and Acronyms

APD	= action potential duration
DNA	= deoxyribonucleic acid
$I_{Cl(Ca)}$	= Ca^{2+} -activated chloride current
I_{Kr}	= fast component of the delayed rectifier potassium current
I_{Ks}	= slow component of the delayed rectifier potassium current
I_{Na-Ca}	= Na^+/Ca^{2+} exchange current
LQTS	= long QT syndrome
LZ	= leucine zipper
PCR	= polymerase chain reaction
TdP	= torsade de pointes
Tpeak-end	= interval between Tpeak and Tend

evaluated in each genotype. Moss et al. (14) have suggested that LQT2 patients with mutations in the pore region of the *KCNH2* gene were at markedly increased risk of arrhythmia-related cardiac events, as compared with patients with non-pore mutations, in the International Long-QT Syndrome Registry. With regard to the LQT1 syndrome, Donger et al. (15) initially suggested that the missense mutation, R555C, located in the C-terminal region of the *KCNQ1* gene was associated with a less severe phenotype than the mutations in the transmembrane regions. Since then, more than 20 mutations located in the C-terminal region of the *KCNQ1* gene have been reported, but neither the severity nor the function of the mutations has been fully determined. In the present study, we compared the arrhythmic risk and sensitivity to sympathetic stimulation with exercise between LQT1 patients with mutations located in the transmembrane regions and those with mutations in the C-terminal regions of the *KCNQ1* gene.

METHODS

Patient population. The study population consisted of 95 patients from 37 unrelated Japanese LQT1 families enrolled from five institutes in Japan: the National Cardiovascular Center, Kyoto University Graduate School of Medicine, Kanazawa University, Niigata University Graduate School of Medical and Dental Science, and Okayama University Graduate School of Medicine and Dentistry. The *KCNQ1* mutations were confirmed in all patients by using standard genetic tests. Briefly, genomic deoxyribonucleic acid (DNA) was isolated from leukocyte nuclei by conventional methods. Screening for mutations of *KCNQ1*, *KCNH2*, *SCN5A*, *KCNE1*, and *KCNE2* was performed by using polymerase chain reaction (PCR)/single-strand conformation polymorphism or denatured high-performance liquid chromatography analyses. For aberrant PCR products, DNA sequencing was conducted with a DNA sequencer (3700 DNA Analyzer, PE Applied Biosystems, Foster City, California). If the patients had double mutations within the *KCNQ1* gene or accompanying additional mutations in other genes, they were excluded from the present study. Genotyping of

LQTS was reviewed and approved according to each Institutional Review Board's guideline, and written, informed consent was obtained from all patients. No patients were taking beta-blockers at the time of the baseline ECG and exercise treadmill test.

Clinical characterization. Routine clinical and ECG parameters were usually obtained at the time of first admission to each institute for evaluation of LQTS, and thereafter at the time of at least yearly follow-up contact.

CLINICAL DIAGNOSIS. We evaluated two major clinical ECG criteria for diagnosing LQTS-affected individuals. The ECG diagnostic criteria of Keating et al. (16), included a corrected QT (QTc) interval ≥ 470 ms in asymptomatic individuals and a QTc interval >440 ms for males and >460 ms for females, were associated with one or more of the following: 1) stress-related syncope; 2) documented TdP; or 3) a family history of early sudden cardiac death. The LQTS was also diagnosed by the diagnostic criteria (score ≥ 4) of Schwartz et al. (17).

BASELINE 12-LEAD ECG MEASUREMENTS. Baseline 12-lead ECG parameters included the RR, Q-Tend, Q-Tpeak, and Tpeak-end (Q-Tend - Q-Tpeak) intervals as an index of transmural dispersion of repolarization. The Q-Tend, Q-Tpeak, and Tpeak-end intervals were also corrected using Bazett's method. These parameters were measured manually in three leads (II, V₂, and V₅), with quantitative repolarization values reported for lead V₅, because the measurements were similar in all three leads. Q-Tend was defined as the interval between the QRS onset and the point at which an isoelectric line intersected a tangential line drawn at the minimum first derivative (dV/dt) point of the positive T-wave or at the maximum dV/dt point of the negative T-wave. When a bifurcated or secondary T wave fusing the first component appeared, it was included as part of the measurement of Q-Tend, but a normal U-wave, which was apparently separated from a T-wave, was not included. Q-Tpeak was defined as the interval between the QRS onset and the peak of the positive T-wave or the nadir of the negative T-wave. Measurements were carried out by two investigators who were unaware of the subjects' genetic status. There were no significant differences in the measured data between the two (data not shown). In addition, TdP and T-wave alternans on the ECG were assessed.

CARDIAC EVENTS, THERAPY, AND FOLLOW-UP. Congenital LQTS-related cardiac events were defined as syncope, aborted cardiac arrest, or unexpected sudden cardiac death without a known cause. Cardiac events, which brought the probands to medical attention but were secondary to apparent causes known to prolong repolarization, such as antiarrhythmic drugs, electrolyte abnormalities, or bradycardia, were excluded from the analysis of congenital LQTS-related cardiac events. Such secondary cardiac events were documented in one patient with C-terminal mutation (hypokalemia 1) and one patient with transmembrane mutation

(hypokalemia 1). Therapy, including beta-blockers, pacemakers, sympathectomy, and defibrillator, was also evaluated. Follow-up was censored at age 50 years to avoid the influence of coronary artery disease on cardiac events in the Japanese population.

EXERCISE TREADMILL TESTING. Forty-nine of the 95 patients were included for the analysis with exercise treadmill testing. All patients were in sinus rhythm, and none had atrioventricular or bundle branch block during the exercise testing. Exercise treadmill testing was performed using the standard Bruce protocol. Twelve-lead ECGs were recorded every 1 min from the baseline condition through the maximal exercise to the recovery phase for 8 min. The ECG measurements before exercise were obtained in the standing position before exercise, and those after exercise were usually obtained within 2 min after stopping exercise to avoid noise in the measurement.

Genetic characterization. Genetic mutations of the *KCNQ1* amino acid sequence were characterized by a specific location and coding effect (missense, splice site, frameshift, or deletion). The transmembrane regions were defined as six transmembrane segments (S1 to S6, amino acid residues 112 through 354), including cytoplasmic and extracellular linkers as well as the pore region. The pore region of the *KCNQ1* channel was defined as the area extending from S5 to the mid-portion of S6 involving amino acid residues 301 through 320.

Statistical analysis. Data are expressed as the mean value \pm SD. Repeated measures two-way analysis of variance (ANOVA), followed by the Scheffé test, was used to compare data between mutations located in the transmembrane regions and those in the C-terminal regions, as well as to compare measurements made before and after exercise (STATISTICA, 1998 edition). Repeated measures one-way ANOVA, followed by the Scheffé test, was used to compare changes (Δ) in the measurements with exercise between the groups. Differences in frequencies were analyzed by the chi-square test. A two-sided p value <0.05 was considered to indicate significance. The cumulative probability of a first cardiac event was assessed by the Kaplan-Meier method and log-rank statistic. The multivariate Cox proportional hazards survivorship model (adjusting for mutation locations, age, and gender) was used to evaluate the independent contribution of clinical and genetic factors to first cardiac events from birth through to age 50 years. Clinical data were also compared between transmembrane mutations and C-terminal mutations for the probands and non-probands, separately. Because the non-probands (family members) in this study were mainly relatives in the first or second degree of the probands, the non-probands in each family were equally handled in the analysis.

RESULTS

Genetic characteristics. Table 1 illustrates the numbers of LQT1 patients by mutation and location (18-24). We

identified 27 *KCNQ1* mutations among the 95 LQT1 patients, with 19 mutations located in the transmembrane regions and eight mutations in the C-terminal regions. Four mutations were located at the pore region in the transmembrane domain. Twenty-three of the 27 mutations were missense mutations; 2 were frameshift mutations; 1 was a deletion mutation; and 1 was a splice mutation. Thirteen mutations (seven in the transmembrane regions and six in the C-terminal regions) were novel. Functional effects by cellular electrophysiologic tests have been reported in eight of the 27 mutations (Table 1).

Clinical characteristics. Sixty-six patients from 27 unrelated families had mutations located in the transmembrane regions, and 29 patients from 10 unrelated families had mutations located in the C-terminal regions. Table 2 illustrates the clinical characteristics of the patient population. No significant differences were observed with regard to gender, percentage of proband, and age at baseline ECG recordings. The LQTS-affected individuals were more frequently diagnosed in patients with transmembrane mutations than in those with C-terminal mutations. The LQTS diagnostic score of Schwartz et al. (17) was significantly higher in patients with transmembrane mutations. The Q-Tend, Q-Tpeak, and Tpeak-end intervals, both uncorrected and corrected, were significantly greater in patients with transmembrane mutations than in those with C-terminal mutations (Figs. 1A and 1C). Although the frequency of TdP was no different, that of T-wave alternans was higher in patients with transmembrane mutations. Patients with transmembrane mutations had more frequent LQTS-related cardiac events (all cardiac events, syncope, and aborted cardiac arrest or unexpected sudden cardiac death) than did those with C-terminal mutations. More therapy with beta-blockers for LQTS was initiated in patients with transmembrane mutations.

Clinical course by mutation location. Figure 2A illustrates Kaplan-Meier cumulative cardiac event curves from birth through to age 50 years for a total of 95 patients with mutations located in the transmembrane regions ($n = 66$) and C-terminal regions ($n = 29$). The difference in the clinical course by mutation location was significant (log-rank, $p = 0.005$), with a greater risk of first cardiac events in patients with transmembrane mutations than in those with C-terminal mutations. Most of the first cardiac events occurred before age 15 years in LQT1 patients with transmembrane mutations, whereas half of the LQT1 patients with C-terminal mutations had their first cardiac events after age 15 years. Multivariate Cox proportional hazards regression analysis revealed that patients with transmembrane mutations had a greater risk of first cardiac events, with a hazard ratio of 3.4 (95% confidence interval 1.4 to 8.2, $p = 0.006$). The corrected Q-Tend modulated the risk among patients with transmembrane mutations, with an 8% increase in risk per 10-ms increase in corrected Q-Tend, but had no effect on risk among patients with C-terminal mutations. Figures 2B and 2C illustrate Kaplan-

Table 1. *KCNQ1* Mutations by Location, Amino-Acid Coding, Type of Mutation, and Reported Functional Effects

Location and Coding	No. of Families	No. of Subjects	Position	Exon	Type	Functional Effect in Expression Studies
Transmembrane domains						
Pore region						
G306R	1	2	Pore	6	Missense	Dominant negative (18)
I313K*	1	1	Pore	7	Missense	
G314A*	1	1	Pore	7	Missense	
G314S	1	1	Pore	7	Missense	
Non-pore region						
R174H	1	2	S2/S3	2	Missense	Loss of function (21)
F193L	1	4	S2/S3	3	Missense	
A226V*	1	3	S4	4	Missense	
R237P*	1	1	S4/S5	5	Missense	
R243C	2	4	S4/S5	5	Missense	
R243I*	1	2	S4/S5	5	Missense	
V254M	2	3	S4/S5	5	Missense	
R259C	1	1	S4/S5	5	Missense	
G269S	3	6	S5	6	Missense	
S277L*	2	4	S5	6	Missense	
G325R	1	4	S6	7	Missense	Loss of function (18)
delF339	1	2	S6	7	Deletion	
A341V	4	19	S6	7	Missense	
A344sp	1	4	S6	7	Splice site	
A344E*	1	2	S6	7	Missense	
C-terminus region						
R451Q*	1	1	C-term.	10	Missense	Trafficking abnormality (24)
I517F*	1	3	C-term.	12	Missense	
A525V*	2	2	C-term.	12	Missense	
L572fs/20*	1	3	C-term.	14	Frameshift	
T587M	2	2	C-term.	15	Missense	
R591H	1	6	C-term.	15	Missense	
D611Y*	1	10	C-term.	16	Missense	
H637fs/28*	1	2	C-term.	16	Frameshift	

*Novel mutation.

del = deletion; sp = last unaffected amino acid before predicted splice mutation; fs = first amino acid affected by a frameshift (number after fs is number of amino acids before termination); term. = terminus.

Meier cumulative cardiac event curves for 37 probands and 58 non-probands with transmembrane mutations and C-terminal mutations, respectively. The difference in phenotype severity based on mutation location persisted ($p = 0.007$) in the non-probands. There was no significant difference in the clinical course of the probands according to mutation site, although the number of probands was relatively small.

Exercise treadmill testing. Exercise treadmill testing was conducted in 33 patients with transmembrane mutations and 16 patients with C-terminal mutations. Table 3 illustrates the ECG measurements before and after exercise testing in both patient groups. The baseline RR and corrected repolarization parameters before exercise in both groups showed quite similar values to those evaluated in the total patients (Table 2), indicating that these patients who had exercise testing were representative of each group. The RR interval was similarly shortened with exercise between the two groups. Exercise produced a significant prolongation in the corrected Q-Tend interval, but not at all in corrected Q-Tpeak, resulting in a significant increase in corrected Tpeak-end in both groups. These changes were much more pronounced in patients with transmembrane

mutations than in those with C-terminal mutations (Figs. 1B and 1D). Therefore, the increases in the corrected Q-Tend and corrected Tpeak-end intervals with exercise were significantly greater in patients with transmembrane mutations (Table 3).

When we re-analyzed the ECG measurements for the probands ($n = 26$) and for the non-probands ($n = 23$) separately, the corrected Q-Tend intervals both before and after exercise were longer in the probands than in the non-probands. However, the magnitude of differences in corrected Q-Tend for the two mutation groups persisted after this re-analysis both in the probands and non-probands (data not shown).

DISCUSSION

The major findings of the present study are: 1) LQT1 patients with mutations located in the transmembrane regions are at a higher risk of congenital LQTS-related cardiac events than are patients with C-terminal mutations; and 2) LQT1 patients with transmembrane mutations had a greater sensitivity to sympathetic stimulation than did patients with C-terminal mutations.

Table 2. Clinical Characteristics of the Study Population

	Transmembrane Domain (n = 66)	C-Terminal (n = 29)	p Value
Demographics			
Female gender (%)	41 (62%)	14 (48%)	NS
Proband (%)	29 (44%)	8 (28%)	NS
Age (yrs) at ECG (range)	32 ± 20 (6-83)	28 ± 17 (4-64)	NS
Diagnosis			
Diagnosed LQTS (Keating)	54 (82%)	7 (24%)	< 0.0001
Diagnosed LQTS (Schwartz >4)	43 (65%)	5 (17%)	< 0.0001
Schwartz score	4.4 ± 2.1	2.0 ± 1.5	< 0.0001
Baseline ECG measurements			
RR (ms)	910 ± 127	918 ± 131	NS
Q-T _{end} (ms)	472 ± 54	419 ± 46	< 0.0001
Q-T _{peak} (ms)	382 ± 46	349 ± 44	0.002
T _{peak-end} (ms)	90 ± 20	71 ± 12	< 0.0001
Corrected Q-T _{end} (ms)	496 ± 46	439 ± 38	< 0.0001
Corrected Q-T _{peak} (ms)	402 ± 42	365 ± 39	0.0002
Corrected T _{peak-end} (ms)	95 ± 19	74 ± 11	< 0.0001
Torsade de pointes (%)	10 (15%)	2 (7%)	NS
T-wave alternans (%)	10 (15%)	0	0.03
Cardiac events			
All cardiac events (%)	36 (55%)	6 (21%)	0.002
Age (yrs) at first events (range)	11 ± 8 (3-48)	13 ± 9 (2-25)	NS
Syncope (%)	36 (55%)	6 (21%)	0.002
Aborted cardiac arrest/SCD (%)	10 (15%)	0	0.03
Therapy			
Beta-blockers (%)	30 (45%)	6 (21%)	0.02
Pacemakers (%)	1 (2%)	0	NS
Sympathectomy (%)	0	0	NS
Defibrillator (%)	0	0	NS

Data are presented as the mean value ± SD or number (%) of subjects.
 ECG = electrocardiography; LQTS = long QT syndrome; SCD = sudden cardiac death.

Mutation site-specific arrhythmic risk in LQT1 syndrome. Moss et al. (14) have recently reported that the greater risk of arrhythmia-related cardiac events in LQT2 patients with pore mutations of the *KCNH2* gene was consistent with the cellular electrophysiologic effects of the *KCNH2* mutations, with pore mutations showing a greater negative effect on the rapidly activating component of the delayed rectifier potassium current (I_{Kr}) than non-pore mutations. Although the cellular electrophysiologic effects of a small percentage of known *KCNQ1* mutations have been reported to be like those of *KCNH2* mutations, several in vitro electrophysiologic studies have reported missense mutations with dominant-negative effects on I_{Ks} in the transmembrane regions of the *KCNQ1* gene (18,19,25,26). However, Wang et al. (18) have suggested that the degree of I_{Ks} suppression by *KCNQ1* transmembrane mutations evaluated in the heterologous expression system did not correlate with severity in the clinical phenotype in LQT1 patients. There have been fewer reports on the cellular electrophysiologic effects of the C-terminal mutations of the *KCNQ1* gene. To the best of our knowledge, the electrophysiologic effects were examined in seven C-terminal mutations of the *KCNQ1* gene (R555C, R533W, R539W, Δ544, G589D, T587M, and G643S) by French, Finland, and Japanese groups (19,20,24,27-30). All seven C-terminal mutations, except for Δ544 and T587M, when

co-expressed with *KCNE1*, could produce functional heteromultimeric channels and showed only a mild reduction of I_{Ks} due to a rightward voltage shift in the activation process and/or acceleration of the deactivation kinetics. Neyroud et al. (28) have reported a homozygous deletion-insertion mutation in the C-terminal region of the *KCNQ1* gene (Δ544), causing a severe phenotype—the Jervell and Lange-Nielsen syndrome. However, the heterozygotes of Δ544 clinically displayed mild or no QT prolongation, with no symptoms, mainly due to the lower dominant-negative effects of the Δ544 mutant. More recently, Larsen et al. (31) have described a severe form of Romano-Ward syndrome associated with compound heterozygosity for two C-terminal mutations (R518X and A525T) in the *KCNQ1* gene. Once again, none of the heterozygotes of the C-terminal mutations (R518X or A525T) had symptoms with minor or no QT prolongation. These previous reports on C-terminal mutations in the *KCNQ1* gene indicate a less severe phenotype in C-terminal mutations than that in transmembrane mutations in LQT1 syndrome, concordant with the findings in the present study.

It is noteworthy that most of the first cardiac events occurred before age 15 years in the LQT1 patients with transmembrane mutations, whereas half of the LQT1 patients with C-terminal mutations had their first cardiac events after age 15 years. This tendency holds up regardless

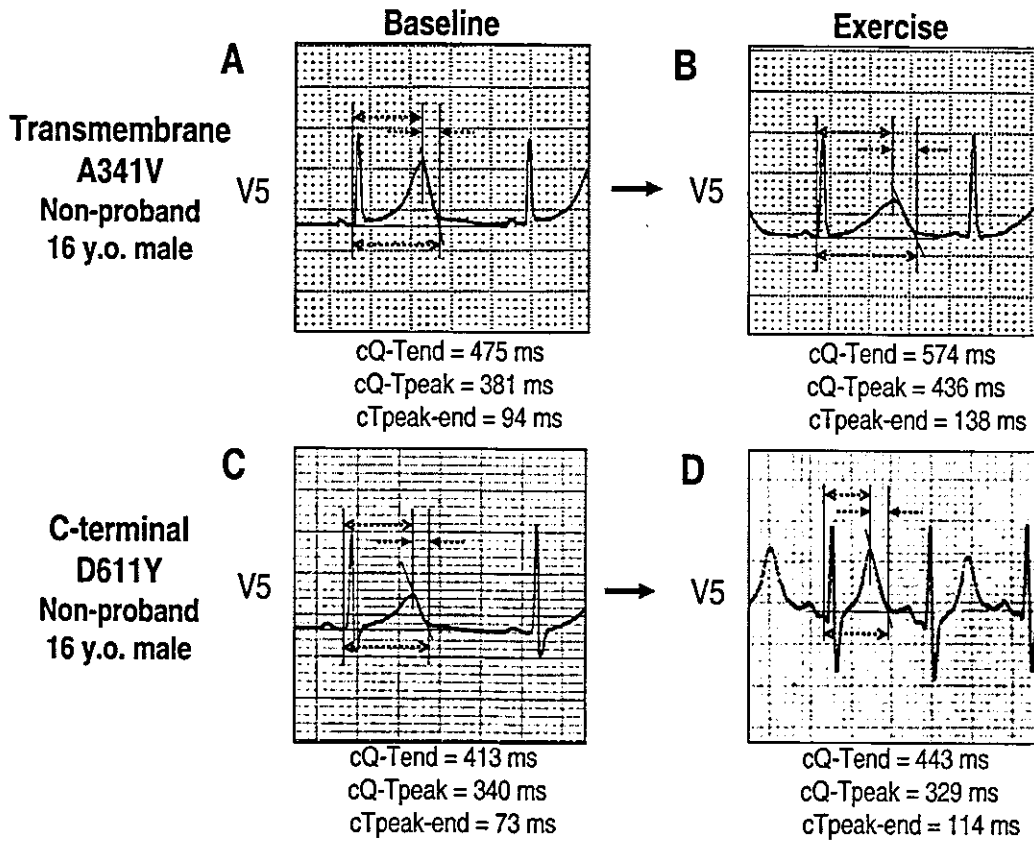


Figure 1. Electrocardiographic parameters in lead V₅ before and after exercise in LQT1 patients with mutations located in the transmembrane region (A341V, non-proband, 16-year-old male) (A and B) and in the C-terminal region (D611Y, non-proband, 16-year-old male) (C and D). The baseline corrected Q-Tend (cQ-Tend), Q-Tpeak (cQ-Tpeak), and Tpeak-end (cTpeak-end) intervals were greater in the patient with a transmembrane mutation than in the patient with a C-terminal mutation (A and C). Exercise produced more prominent increases in the cQ-Tend and cTpeak-end in the patient with a transmembrane mutation than in the patient with a C-terminal mutation (B and D).

of whether the patient was a proband. Moreover, hypokalemia, which is known to prolong repolarization, unmasked the LQTS proband in a patient with C-terminal mutation in the present study. These findings suggest that careful

follow-up is needed in LQT1 patients with C-terminal mutations, despite their less severe phenotype, by limiting exposure of these patients to QT prolonging conditions.

Although the difference in the clinical course based on

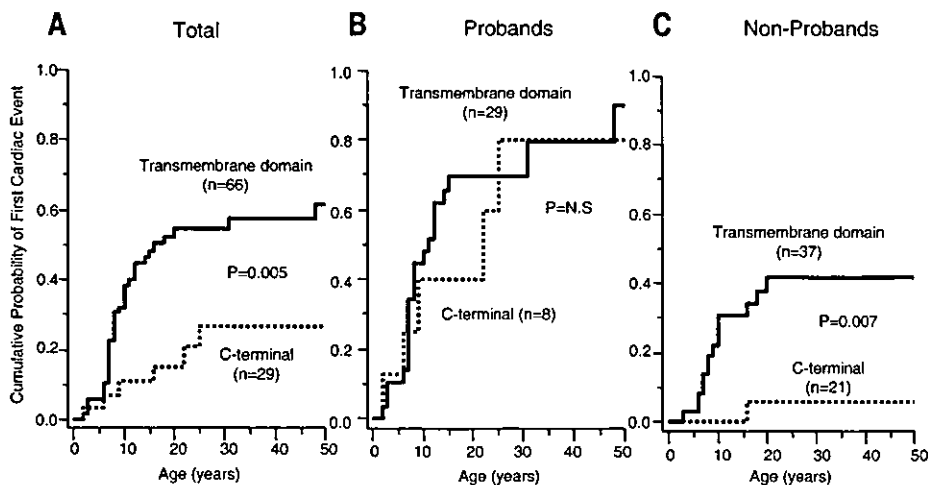


Figure 2. (A) Kaplan-Meier cumulative cardiac event curves from birth through to age 50 years for a total of 95 patients with *KCNQ1* mutations located in the transmembrane regions (n = 66) and C-terminal regions (n = 29). The difference in the clinical course by mutation location was significant (log-rank, p = 0.005), with a greater risk of first cardiac events in patients with transmembrane mutations than in those with C-terminal mutations. Kaplan-Meier cumulative cardiac event curves for 37 probands (B) and 58 non-probands (C) with transmembrane mutations and C-terminal mutations.

Table 3. Electrocardiographic Measurements Before and After Exercise Testing

	Transmembrane Domain (n = 33)	C-Terminal (n = 16)	p Value
Demographics			
Female gender (%)	18 (55%)	7 (44%)	NS
Proband (%)	22 (67%)	4 (25%)	0.006
Age (yrs) at ECG (range)	26 ± 16 (9-72)	27 ± 13 (6-45)	NS
ECG measurements before exercise			
RR (ms)	862 ± 128	850 ± 106	NS
Corrected Q-T _{end} (ms)	494 ± 40	435 ± 28	<0.0001
Corrected Q-T _{peak} (ms)	403 ± 37	359 ± 26	<0.0001
Corrected T _{peak-end} (ms)	91 ± 12	76 ± 6	NS
ECG measurements after exercise			
RR (ms)	514 ± 87*	503 ± 74*	NS
Corrected Q-T _{end} (ms)	571 ± 45*	470 ± 39*	<0.0001
Corrected Q-T _{peak} (ms)	420 ± 38	365 ± 51	<0.0001
Corrected T _{peak-end} (ms)	151 ± 34*	106 ± 17*	<0.0001
Changes in ECG measurements with exercise			
RR (ms)	349 ± 119	348 ± 137	NS
Corrected Q-T _{end} (ms)	77 ± 32	35 ± 17	<0.0001
Corrected Q-T _{peak} (ms)	17 ± 36	5 ± 30	NS
Corrected T _{peak-end} (ms)	60 ± 34	30 ± 17	0.002

*p < 0.005 vs. before exercise. Data are presented as the mean ± SD value or number (%) of subjects. The electrocardiographic (ECG) measurements after exercise were obtained within 2 min after stopping exercise.

mutation location was obvious in the non-probands, no significant difference was observed in the clinical course according to mutation location in the probands. This is not surprising, because probands are usually brought to medical attention by their first cardiac events, especially those with a less prolonged QT interval. There indeed may be no difference in cardiac events based on mutation location for probands. This is because other modifier genes may be contributing to the more severe phenotype, which leads to the individual receiving a label of "proband."

Zareba et al. (32) recently reported on 294 LQT1 patients in the International Long-QT Syndrome Registry and analyzed the QTc interval and cardiac event rates by mutation location. In contrast to the present study, they found no significant differences in QTc or risk of cardiac events when the patients were separated into those with transmembrane mutations and those with C-terminal mutations. However, only six transmembrane mutations were overlapped between the two studies (out of 31 transmembrane mutations in the Registry and 19 transmembrane mutations in this study). Moreover, no overlap was observed in the C-terminal mutations between the two studies (out of 11 C-terminal mutations in the Registry and 8 C-terminal mutations in this study). In transmembrane regions, the S4 to S5 loop (amino acid residues 221 through 300) and the S6 segment (amino acid residues 325 through 354) are known to be important for voltage-dependent I_{Ks} function (22); thus, a more severe phenotype is expected in mutations located in the S4 to S5 loop and the S6 segment than in the S2 to S3 loop (amino acid residues 148 through 220). The transmembrane mutations in the non-pore region in the present study were located in the S4 to S5 loop and the S6 segment, except for two mutations found in the S2 to S3

loop. This may affect the result that cardiac event rates were higher in patients with transmembrane mutations in the present study than those in the Registry. Interestingly, when the patients with transmembrane mutations in the present study were separated into those with pre-pore mutations and those with pore mutations, according to the definition by Zareba et al. (32), the patients with pore mutations had a longer corrected Q-Tend than did those with pre-pore mutations (data not shown). Overall, our data present evidence that mutation site-specific differences in arrhythmic risk exist, in contrast to findings previously reported from the Long-QT Syndrome Registry. Therefore, a larger patient population per mutation and a greater spectrum of *KCNQ1* mutations by corroboration with other investigators are clearly needed to make a definitive conclusion about the mutation site-specific differences in arrhythmic risk in LQT1 syndrome.

Greater sensitivity to sympathetic stimulation in transmembrane mutations of the *KCNQ1* gene. The LQT1 syndrome is reported both clinically and experimentally to be the most sensitive to sympathetic stimulation among the seven forms of LQTS (9-12). Sympathetic stimulation is known to increase the net outward repolarizing current due to a larger increase in outward currents, including Ca²⁺-activated I_{Ks} and Ca²⁺-activated chloride current (I_{Cl(Ca)}), compared with the inward Na⁺/Ca²⁺ exchange current (I_{Na-Ca}), resulting in an abbreviation of action potential duration (APD) and QT interval under normal conditions. A defect in I_{Ks} in LQT1 syndrome could account for the failure of sympathetic stimulation to abbreviate the QT interval and APD, especially in the mid-myocardial regions, resulting in a paradoxical QT prolongation and an increase in transmural dispersion of repolarization reflecting an

increase in the Tpeak-end interval under sympathetic stimulation (12). In fact, recent clinical studies have demonstrated that sympathetic stimulation with epinephrine infusion or exercise produced a more significant increase in Q-Tend and Tpeak-end intervals in LQT1 compared with LQT2 patients (33-35). More recently, the Q-Tend and Tpeak-end intervals both before and after epinephrine and prolongation of Q-Tend with epinephrine were reported to be greater in symptomatic than asymptomatic patients with LQT1 syndrome (9). In the present study, LQT1 patients with transmembrane mutations, who had more frequent LQTS-related cardiac events than those with C-terminal mutations, showed greater baseline Q-Tend and Tpeak-end intervals and a greater increase in both Q-Tend and Tpeak-end intervals with exercise than those with C-terminal mutations. The data in the present study may indicate a stricter exercise limit and a more aggressive use of beta-blockers in LQT1 patients with transmembrane mutations, but once again, we need to evaluate a larger patient population to make a definitive recommendation.

With regard to the sympathetic regulation of I_{Ks} , Marx et al. (36) have suggested that beta-adrenergic modulation of I_{Ks} required targeting of cyclic adenosine monophosphate (cAMP)-dependent protein kinase and protein phosphatase-1 to *KCNQ1* through the targeting protein yotiao. The binding of protein kinase and protein phosphatase-1 to the *KCNQ1* channel through yotiao is mediated by leucine zipper (LZ) motifs located in the C-terminal of the *KCNQ1* gene (amino acid residues 588 to 616). They also reported that the G589D mutant channel located in the LZ motifs of the C-terminus prevented cAMP-dependent regulation of I_{Ks} , and thus may not respond to beta-adrenergic stimulation, resulting in a defect of APD shortening and further prolonging of the APD. The G589D mutation was not included among the C-terminal mutations of the present study. Two C-terminal mutations, R591H and D611Y, located in the LZ motifs were included in the present study. However, the prolongation of the QTc interval was mild in patients with the two mutations (Fig. 1). Further clinical evaluation will be required to conclude the role of LZ motifs in the C-terminus on sympathetic modulation of the I_{Ks} channel.

Acknowledgments

We gratefully acknowledge the expert technical assistance of Naotaka Ohta and Ritsuko Yamamoto (Laboratory of Molecular Genetics, National Cardiovascular Center, Suita, Japan).

Reprint requests and correspondence: Dr. Wataru Shimizu, Division of Cardiology, Department of Internal Medicine, National Cardiovascular Center, 5-7-1 Fujishiro-dai, Suita, Osaka, 565-8565 Japan. E-mail: wshimizu@hsp.ncvc.go.jp.

REFERENCES

- Schwartz PJ, Periti M, Malliani A. The long QT syndrome. *Am Heart J* 1975;89:378-90.

- Moss AJ, Schwartz PJ, Crampton RS, et al. The long QT syndrome: a prospective international study. *Circulation* 1985;71:17-21.
- Keating MT, Sanguinetti MC. Molecular and cellular mechanisms of cardiac arrhythmias. *Cell* 2001;104:569-80.
- Plaster NM, Tawil R, Tristani-Firouzi M, et al. Mutations in Kir2.1 cause the developmental and episodic electrical phenotypes of Andersen's syndrome. *Cell* 2001;105:511-9.
- Mohler PJ, Schott JJ, Gramolini AO, et al. Ankyrin-B mutation causes type 4 long-QT cardiac arrhythmia and sudden cardiac death. *Nature* 2003;421:634-9.
- Splawski I, Shen J, Timothy KW, et al. Spectrum of mutations in long-QT syndrome genes: KVLQT1, HERG, SCN5A, KCNE1, and KCNE2. *Circulation* 2000;102:1178-85.
- Sanguinetti MC, Curran ME, Zou A, et al. Coassembly of KvLQT1 and minK (IsK) proteins to form cardiac I_{Ks} potassium channel. *Nature* 1996;384:80-3.
- Priori SG, Napolitano C, Schwartz PJ. Low penetrance in the long-QT syndrome: clinical impact. *Circulation* 1999;99:529-33.
- Shimizu W, Noda T, Takaki H, et al. Epinephrine unmasks latent mutation carriers with LQT1 form of congenital long QT syndrome. *J Am Coll Cardiol* 2003;41:633-42.
- Priori SG, Schwartz PJ, Napolitano C, et al. Risk stratification in the long-QT syndrome. *N Engl J Med* 2003;348:1866-74.
- Schwartz PJ, Priori SG, Spazzolini C, et al. Genotype-phenotype correlation in the long-QT syndrome: gene-specific triggers for life-threatening arrhythmias. *Circulation* 2001;103:89-95.
- Shimizu W, Antzelevitch C. Cellular basis for the electrocardiographic features of the LQT1 form of the long QT syndrome: effects of beta-adrenergic agonists, antagonists and sodium channel blockers on transmural dispersion of repolarization and torsade de pointes. *Circulation* 1998;98:2314-22.
- Zareba W, Moss AJ, Schwartz PJ, et al. Influence of the genotype on the clinical course of the long-QT syndrome. *N Engl J Med* 1998;339:960-5.
- Moss AJ, Zareba W, Kaufman ES, et al. Increased risk of arrhythmic events in long-QT syndrome with mutations in the pore region of the human ether-a-go-go-related gene potassium channel. *Circulation* 2002;105:794-9.
- Donger CD, Denjoy I, Berthet M, et al. *KVLQT1* C-terminal missense mutation causes a forme fruste long-QT syndrome. *Circulation* 1997;96:2778-81.
- Keating M, Atkinson D, Dunn C, et al. Linkage of a cardiac arrhythmia, the long QT syndrome, and the Harvey ras-1 gene. *Science* 1991;252:704-6.
- Schwartz PJ, Moss AJ, Vincent GM, et al. Diagnostic criteria for the long QT syndrome: an update. *Circulation* 1993;88:782-4.
- Wang Z, Tristani-Firouzi M, Xu Q, et al. Functional effects of mutations in KvLQT1 that cause long QT syndrome. *J Cardiovasc Electrophysiol* 1999;10:817-26.
- Chouabe C, Neyroud N, Guicheney P, et al. Properties of KvLQT1 K⁺ channel mutations in Romano-Ward and Jervell and Lange-Nielsen inherited cardiac arrhythmias. *EMBO J* 1997;16:5472-9.
- Mohammad-Panah R, Demolombe S, Neyroud N, et al. Mutations in a dominant-negative isoform correlate with phenotype in inherited cardiac arrhythmias. *Am J Hum Genet* 1999;64:1015-23.
- Yamaguchi M, Shimizu M, Ino H, et al. Clinical and electrophysiological characterization of a novel mutation (F193L) in the *KCNQ1* gene associated with long QT syndrome. *Clin Sci* 2003;104:377-82.
- Franquez L, Lin M, Shen J, et al. Long QT syndrome-associated mutations in the S4-S5 linker of KvLQT1 potassium channels modify gating and interaction with minK subunits. *J Biol Chem* 1999;274:21063-70.
- Kubota T, Shimizu W, Kamakura S, et al. Hypokalemia-induced long QT syndrome with an underlying novel missense mutation in S4-S5linker of *KCNQ1*. *J Cardiovasc Electrophysiol* 2000;11:1048-54.
- Yamashita F, Horie M, Kubota T, et al. Characterization and subcellular localization of *KCNQ1* with a heterozygous mutation in the C terminus. *J Mol Cell Cardiol* 2001;33:197-207.
- Wang Q, Curran ME, Splawski I, et al. Positional cloning of a novel potassium channel gene: *KVLQT1* mutations cause cardiac arrhythmias. *Nat Genet* 1996;12:17-23.
- Shalaby FY, Levesque PC, Yang WP, et al. Dominant-negative KvLQT1 mutations underlie the LQT1 form of long QT syndrome. *Circulation* 1997;96:1733-6.

27. Chouabe C, Neyroud N, Richard P, et al. Novel mutations in KvLQT1 that affect I_{ks} activation through interactions with Isk. *Cardiovasc Res* 2000;45:971–80.
28. Neyroud N, Tesson F, Leibovici M, et al. A novel mutation in the potassium channel gene *KVLQT1* caused the Jervell and Lange-Nielsen cardioauditory syndrome. *Nat Genet* 1997;15:186–9.
29. Piippo K, Swan H, Pasternack M, et al. A founder mutation of the potassium channel *KCNQ1* in long QT syndrome: implications for estimation of disease prevalence and molecular diagnostics. *J Am Coll Cardiol* 2001;37:562–8.
30. Kubota T, Horie M, Takano M, et al. Evidence for a single nucleotide polymorphism in the *KCNQ1* potassium channel that underlies susceptibility to life-threatening arrhythmias. *J Cardiovasc Electrophysiol* 2001;12:1223–9.
31. Larsen LA, Fosdal I, Andersen PS, et al. Recessive Romano-Ward syndrome associated with compound heterozygosity for two mutations in the *KVLQT1* gene. *Eur J Hum Genet* 1999;7:724–8.
32. Zareba W, Moss AJ, Sheu G, et al. Location of mutation in the *KCNQ1* and phenotypic presentation of long QT syndrome. *J Cardiovasc Electrophysiol* 2003;14:1149–53.
33. Ackerman MJ, Khositseth A, Tester DJ, et al. Epinephrine-induced QT interval prolongation: a gene-specific paradoxical response in congenital long QT syndrome. *Mayo Clin Proc* 2002;77:413–21.
34. Shimizu W, Tanabe Y, Aiba T, et al. Differential effects of β -blockade on dispersion of repolarization in absence and presence of sympathetic stimulation between LQT1 and LQT2 forms of congenital long QT syndrome. *J Am Coll Cardiol* 2002;39:1984–91.
35. Takenaka K, Ai T, Shimizu W, et al. Exercise stress test amplifies genotype-phenotype correlation in the LQT1 and LQT2 forms of the long QT syndrome. *Circulation* 2003;107:838–44.
36. Marx SO, Kurokawa J, Reiken S, et al. Requirement of a macromolecular signaling complex for beta-adrenergic receptor modulation of the *KCNQ1-KCNE1* potassium channel. *Science* 2002;295:496–9.

Additional Gene Variants Reduce Effectiveness of Beta-Blockers in the LQT1 Form of Long QT Syndrome

ATSUSHI KOBORI, M.D.,* NOBUAKI SARAI, M.D.,† WATARU SHIMIZU, M.D., PH.D.,‡
 YOSHIHIDE NAKAMURA, M.D.,§ YOSUKE MURAKAMI, M.D.,¶
 TAKERU MAKIYAMA, M.D.,* SEIKO OHNO, M.D.,* KOTOE TAKENAKA, M.D.,*
 TOMONORI NINOMIYA, M.D.,* YUICHIRO FUJIWARA, M.D.,|| SATOSHI MATSUOKA, M.D.,
 PH.D.,† MAKOTO TAKANO, M.D., PH.D.,† AKINORI NOMA, M.D., PH.D.,†
 TORU KITA, M.D., PH.D.,* and MINORU HORIE, M.D., PH.D.**

From the Departments of *Cardiovascular Medicine and †Physiology and Biophysics, Kyoto University Graduate School of Medicine, Kyoto, Japan; ‡Division of Cardiology, Department of Internal Medicine, National Cardiovascular Center, Osaka, Japan; §Department of Pediatric Cardiology, Japanese Red Cross Society Wakayama Medical Center, Wakayama, Japan; ¶Department of Pediatric Cardiology, Osaka City General Hospital, Osaka, Japan; ||Department of Physiology, Tokyo Medical and Dental University, Tokyo, Japan; **Department of Cardiovascular and Respiratory Medicine, Shiga University of Medical Science, Shiga, Japan

Additional Mutations in LQT1. Introduction: Beta-blockers are widely used to prevent the lethal cardiac events associated with the long QT syndrome (LQTS), especially in *KCNQ1*-related LQTS (LQT1) patients. Some LQT1 patients, however, are refractory to this therapy.

Methods and Results: Eighteen symptomatic LQTS patients (12 families) were genetically diagnosed as having heterozygous *KCNQ1* variants and received beta-blocker therapy. Cardiac events recurred in 4 members (3 families) despite continued therapy during mean follow-up of 70 months. Three of these patients (2 families) had the same mutation [A341V (*KCNQ1*)] and the other had R243H (*KCNQ1*). The latter patient took aprindine, which seemed to be responsible for the event. By functional assay using a heterologous mammalian expression system, we found that A341V (*KCNQ1*) is a loss-of-function type mutation (not dominant negative). Further genetic screening revealed that one A341V (*KCNQ1*) family cosegregated with S706C (*KCNH2*) and another with G144S (*KCNJ2*). Functional assay of the S706C (*KCNH2*) mutation was found to reduce the current density of expressed heterozygous *KCNH2* channels with a positive shift (+8 mV) of the activation curve. Action potential simulation study was conducted based on the KYOTO model to estimate the influence of additional gene modifiers. In both models mimicking LQT1 plus 2 and LQT1 plus 7, the incidence of early afterdepolarization was increased compared with the LQT1 model under the setting of beta-adrenergic stimulation.

Conclusion: Multiple mutations in different LQTS-related genes may modify clinical characteristics. Expanded gene survey may be required in LQT1 patients who are resistant to beta-blocker therapy. (*J Cardiovasc Electrophysiol*, Vol. 15, pp. 190-199, February 2004)

long QT syndrome, beta-blocker, KCNQ1, KCNH2, KCNJ2, computer simulation

Introduction

A number of mutations in genes coding cardiac ion channels delay the repolarization of the ventricle, thereby causing long QT syndrome (LQTS). At least six responsible LQTS-related genes have been identified: *KCNQ1*—LQT1,¹ *KCNH2*—LQT2,² *SCN5A*—LQT3,³

ANKB—LQT4,⁴ *KCNE1*—LQT5,⁵ and *KCNE2*—LQT6.⁶ Another autosomal dominant form of congenital LQTS is accompanied by periodic paralysis and dysmorphic features (Andersen syndrome).⁷ More recently, mutations in *KCNJ2*, which codes cardiac inward rectifier potassium channels (Kir2.1), were found to result in the syndrome (LQT7).^{8,9} Thus, novel knowledge of the genetic aspect of LQTS paved a new path to understanding the mechanism of the disease and choosing gene-specific treatment.^{10,11}

For example, beta-blockers are first-line strategy for treatment of LQTS patients.¹² Such therapy provided >80% effectiveness in LQT1 mutation carriers.^{10,13} In contrast, beta-blockers are not as effective in LQT2 and LQT3 patients (50%–59%),¹⁰ suggesting the genotype-dependent efficacy of the drug. However, some LQT1 patients did not respond to beta-blocker administration and required further conjunctive therapy (pacemaker, implantable cardiac defibrillator). These findings indicate the heterogeneity of the LQT1 patient population.

In the present study, we focused on the prevalence of nonresponders to beta-blockers among genetically diagnosed LQT1 patients and found that additional gene mutations

Dr. Shimizu is supported by the Japanese Cardiovascular Research Foundation, the Vehicle Racing Commemorative Foundation, and by Health Science Research Grants from the Ministry of Health, Labor, and Welfare, Japan. Dr Horie is supported in part by research grants from the Ministry of Education, Science, Sports and Culture of Japan, by the Takeda Foundation for Science Promotion, and by the Japan Heart Foundation/Pfizer Grant for Cardiovascular Disease Research.

Address for correspondence: Minoru Horie, M.D., Ph.D., Department of Cardiovascular and Respiratory Medicine, Shiga University of Medical Science, Seta Tsukinowa-cho, Otsu, Shiga, Japan 520-2192. Fax: 81-77-543-5839; E-mail: horie@belle.shiga-med.ac.jp

Manuscript received 30 April 2003; Accepted for publication 8 October 2003.

doi: 10.1046/j.1540-8167.2004.03112.x

different from those in *KCNQ1* are responsible for generation of the clinical phenotype.

Methods

Study Subjects

Eighteen LQT1 patients from 12 unrelated Japanese families were included in the analysis. As described previously,¹⁴ all represented with (1) unexplained syncope, aborted cardiac arrest requiring cardiac resuscitation, or documented polymorphic ventricular tachycardia (VT; torsades de pointes [TdP]); (2) corrected QT interval for heart rate (QTc) >460 ms; or (3) QTc >440 ms associated with bradycardia or abnormal T wave pattern. QT intervals were measured on baseline ECG in lead II or V₅ and were corrected for heart rate according to Bazett's formula.¹⁵

DNA Isolation and Mutation Analysis

The protocol for genetic analysis was approved by and performed under the guidelines of the Institutional Ethics Committee. All subjects gave informed consent prior to gene analysis. Genomic DNA was isolated from leukocyte nuclei using conventional methods.¹⁶ Genetic screening was performed for *KCNQ1* and other LQTS-related genes (*KCNH2*, *SCN5A*, *KCNE1*, *KCNE2*, *KCNJ2*) using polymerase chain reaction/single-strand conformation polymorphism (PCR-SSCP) analysis.¹⁷ Abnormal conformers were amplified by PCR, and sequencing was performed on an ABI PRISM310 DNA sequencer (Perkin-Elmer Applied Biosystems, Wellesley, MA, USA).

In Vitro Mutagenesis

With regard to the specific *KCNQ1* mutation A341V, site-directed mutagenesis was used to construct the mutant as described previously.¹⁸ Briefly, human *KCNQ1* cDNA (kind gift from Dr. Barhanin) was subcloned into pIRES2-EGFP plasmid (Clontech, Palo Alto, CA, USA). The *KCNQ1* mutant was synthesized by overlap extension at the index site using sequential PCR. Human *KCNH2* cDNA (kind gift from Dr. Sanguinetti) was subcloned into pRc/CMV plasmid (Invitrogen, Carlsbad, CA, USA) as described previously.¹⁷ A specific *KCNH2* mutation, S706C, was constructed from pRc/CMV-*KCNH2* using a site-directed mutagenesis kit (QuikChange II XL, Stratagene, La Jolla, CA, USA). Introduction of the mutation was confirmed by sequencing the mutation primer and the surrounding regions.

Electrophysiologic Experiments and Data Analysis

To assay the functional modulation of *KCNQ1* and *KCNH2*, we used a heterologous expression system using COS7 cell line as previously described.¹⁸ Briefly, the cells were transiently transfected by the LipofectAMINE method according to the manufacturer's instructions (Gibco BRL, Rockville, MD, USA), using 0.5 to 2 μ g/35 mm dish of pIRES2-EGFP/*KCNQ1* or pRc/CMV-*KCNH2* (wild-type [WT] and/or mutant). All experiments were performed in the presence of cotransfection of pIRES2-CD8/*KCNE1* (1 μ g/35-mm dish) with pIRES2-EGFP/*KCNQ1*, or pCI/GFP with pRc/CMV-*KCNH2*. By using both green fluorescent protein (GFP) fluorescence and anti-CD8 antibody-coated beads (Dynabeads CD8, Dynal Biotech, Oslo, Norway), it was possible to select successfully cotransfected cells. The cells were studied by the conventional whole-cell patch clamp technique at 37°C, 48 to 72 hours after transfection. Pipettes were filled with a solution contained (in mM): KCl 130, KOH 20, Mg-ATP 5, Na-GTP 0.1, Na₂-phosphocreatine 5, EGTA 5, and HEPES 5 (pH 7.3 with HCl), and had a resistance of 3.0 to 5.0 M Ω . The solution used to perfuse the cells contained (in mM): NaCl 140, KCl 5.4, MgCl₂ 0.5, CaCl₂ 1.8, NaH₂PO₄ 0.33, glucose 5.5, and HEPES 5 (pH 7.4 with NaOH).¹⁷ All data are given as mean \pm SEM. Where appropriate, Student's unpaired *t*-test was used, *P* < 0.05 was considered statistically significant.

Action Potential Model Simulation

The KYOTO computer model was used to calculate the estimated result on action potentials (APs).¹⁹ In order to mimic the AP characteristics of human mid-myocardial (M) cells in the left ventricle, we changed parameters of major ion currents in the original model¹⁹ according to human experimental data,²⁰⁻²⁷ as summarized in Table 1. For constructing the epicardial (Epi) cell model, we arranged the parameters of the M cell as follows: magnifying current amplitude of the slow component of the delayed rectifier potassium current (*I*_{Ks}) and transient outward potassium current (*I*_{to}) 4 and 1.5 times, respectively.^{22,24} Conduction time between M and Epi was set at 20 ms and extracellular K concentration (*K*⁺) at 4.0 mEq/L.

To simulate the condition of beta-adrenergic stimulation, we set the parameters as previously described²⁸: (1) magnifying *P*_{CaL} 4 times and slowing the time constant of inactivation 1.5 times in L-type calcium current (*I*_{CaL}), (2) magnifying *I*_{Ks} amplitude 4 times with a 8-mV shift of the activation curve in the hyperpolarization direction, (3) magnifying *I*_{max} of the

TABLE 1
Setting Parameters for the Mid-Myocardial (M) Cell Model

Current	Modulation	Reference
<i>I</i> _{CaL}	Calcium-binding rate (<i>k</i> _{U,C} = 0.28, <i>k</i> _{U_{Ca},CCa} = 0.28, <i>k</i> _{CCa,C} = 0.0087)	20
<i>I</i> _{Kr}	<i>V</i> _{1/2} of activation property = -14.4 mV Magnifying <i>G</i> _{Kr} 1.7 times	21
<i>I</i> _{Ks}	<i>V</i> _{1/2} of activation property = 10.0 mV Magnifying current amplitude 1.14 times	22
<i>I</i> _{to}	<i>V</i> _{1/2} of inactivation property = -33.3 mV Magnifying current amplitude 400 times	23 24, 25
<i>I</i> _{K1}	Magnifying <i>G</i> _{K1} 0.7 times	26
<i>I</i> _{Na}	<i>V</i> _{1/2} of ultraslow inactivation property = -87.0 mV	27

*V*_{1/2} = half-maximal activation potential. Other abbreviations as in reference 19.

TABLE 2
Characteristics of LQT1 Patients

Variants in <i>KCNQ1</i>	No. of Kindred	Age/Sex	QTc (ms)	Cardiac Event Before Therapy	Therapy	Follow-Up Period (months)	Recurrence	Additional Mutation
R243H	K-088	52/F	634	+	BB, SCB	31	+	
G314S	K-056	37/F	622	-	BB	36	-	
G314A*	K-020	27/F	610	+	BB	75	-	
A341V	K-024	58/F	500	+	BB	72	-	
		11/M	460	+	BB	53	+	G144S (<i>KCNJ2</i>)
	K-125	36/F	480	+	BB	53	+	
		15/F	560	+	BB	144	+	S706C (<i>KCNH2</i>)
	K-001	39/F	500	+	BB	84	-	
		10/F	488	+	BB	82	-	
		38/F	647	+	BB	180	-	
		10/M	524	+	BB	60	-	
I517T*	K-034	13/M	496	+	BB	108	-	
		13/M	500	+	BB	88	-	
G643S	K-047	45/F	487	+	BB, K	38	-	
	K-057	23/F	470	+	BB	66	-	
	K-071	57/F	502	+	BB, ICD	36	-	
	K-072	30/F	480	+	BB	36	-	
	K-094	23/F	469	+	BB, K	26	-	

*Novel mutations.

BB = Beta-blocker; ICD = implantable cardioverter defibrillator; K = potassium supplement; SCB = sodium channel blocker.

Ca²⁺ pump in sarcoplasmic reticulum and Na⁺/K⁺ pump 1.41 and 1.2 times, respectively, and (4) shifting the fast inactivation curve of the sodium current (I_{Na}) 3.4 mV in the hyperpolarization direction.

Results

Mutation Analysis and General Clinical Findings

Table 2 summarizes mutational and clinical findings. We identified 6 *KCNQ1* variants: 5 missense (including 2 novel, indicated by asterisks) mutations and 1 single nucleotide polymorphism (SNP) in 12 probands. Six family members also were identified as having *KCNQ1* mutations. Eventually, 18 patients were heterozygous and received beta-blocker medication for a mean period of 70.4 ± 9.6 months at the time point of data analysis. Population characteristics were predominantly female (female/male: 14:4) and symptomatic before introduction of beta-blockers (positive/negative: 17:1). Mean age was 29.8 ± 3.8 years, and QTc intervals were 523.8 ± 3.8 ms.

Four of 18 LQT1 patients were nonresponders to beta-blockers (Table 2). With regard to genetic abnormality, 1 had R243H and 3 had A341V *KCNQ1* mutations. The latter was a hot-spot mutation that resulted from C-to-T substitution at position 1022 (Fig. 1A).²⁹ In all patients, extensive genetic analyses also were conducted for the other LQTS-related genes: *KCNH2*, *SCN5A*, *KCNE1*, *KCNE2*, and *KCNJ2*. Three of 4 nonresponders who were carriers of heterozygous A341V were found to have additional mutations: heterozygous *KCNJ2* and *KCNH2* mutations, respectively. The former mutation, G144S (*KCNJ2*), resulted from G-to-A substitution at position 430 (Fig. 1B) and was the same as reported by Plaster et al.⁸ The latter mutation, S706C (*KCNH2*), resulted from G-to-C substitution at position 2117 (Fig. 1C) and was a novel mutation, located between the sixth transmembrane and cyclic nucleotide binding domain.

The remaining 14 patients were all beta-blocker responders, including 2 members of the double-mutation family

discussed earlier (K-125, Table 2). Detailed genetic analyses found no appended mutations in the LQTS-related genes. All mutational changes listed in Table 2 were absent in > 100 controls, except G643S (*KCNQ1*), an SNP common and specific in the Japanese population.³⁰

Case Reports of Nonresponders to Beta-Blockers

A341V (*KCNQ1*)-G144S (*KCNJ2*) family (Table 2, K-024)

A 36-year-old woman (no. 4 in the family tree shown in Fig. 2A-a) and her 11-year-old son (no. 7) were diagnosed as LQT1 plus LQT7 (Andersen syndrome). No other family members were symptomatic (Fig. 2A-a). PCR-SSCP (Fig. 2A-b and 2A-c) revealed that two different mutations in *KCNQ1* and *KCNJ2* were cosegregated only in these two members of the family, suggesting that the mutations are de novo in the mother.

The female patient developed normally until age 12 years, when she first experienced loss of consciousness after swimming and required resuscitation. She was diagnosed with ventricular tachycardia (VT) and began beta-blocker therapy, but she complained of dizziness and recurrent syncope. After genetic diagnosis of LQT1 was made, she was given another beta-blocker (atenolol 50 mg/day) and K⁺ supplement therapy. The syncope and VT decreased, but the faintness and dizziness continued. Baseline ECG showed QT prolongation (QTc = 512 ms) with prominent U waves (Fig. 2B) and incessant bigeminy with multiform premature ventricular complexes (PVC). Since the age of 13 years, she had experienced episodes of muscle weakness 1 to 2 times per month, especially during menstruation, which proved to be independent of serum K⁺ concentration. She had short stature, micrognathia, low-set ears, broad forehead, and scoliosis.

The woman's son was born after a normal pregnancy and delivery. At the age of 1 year, he began to suffer from afebrile seizures and was given valproic acid for several years. Electroencephalographic study performed when he was 5 years old revealed polymorphic VT. After the genetic diagnosis

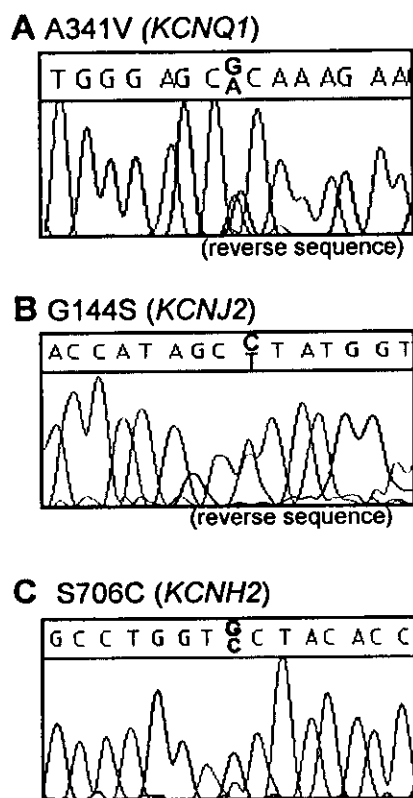


Figure 1. DNA sequences of our mutations. Sequence chromatographs showed heterozygous single base-pair substitutions: (A) C-to-T (G-to-A in reverse sequence) conducted to Ala341Val in *KCNQ1*; (B) G-to-A (C-to-T in reverse sequence) conducted to Gly144Ser in *KCNJ2*; and (C) G-to-C conducted to Ser706Cys in *KCNH2*.

was made, he began taking a beta-blocker (propranolol 30–60 mg/day) at age 7 years. However, at age 10 years he developed syncope during mild exercise that required cardiac resuscitation. ECG showed QT prolongation (QTc = 490 ms), prominent U wave, incessant bigeminy with multiform PVC, and bidirectional VT (Fig. 2C). After aborted sudden death, verapamil was supplemented and was successful in preventing symptomatic events for 2 years. He has complained of easy fatigability but has experienced no major attacks of muscle paralysis. He has the same dysmorphic features, characteristic of Andersen syndrome, as his mother.

A341V (*KCNQ1*)–S706C (*KCNH2*) family (Table 2; K-125)

A 15-year-old girl (no. 2 in the family tree shown in Fig. 3A-a) was a proband and member of a typical LQTS family. Her mother (no. 1 in Fig. 3A-a) and younger sister (no. 3) also were symptomatic and receiving beta-blocker therapy. Several members on the maternal side of her family, except her grandfather, presented with recurrent syncope without available genetic information (gray symbols in Fig. 3A-a).

She developed normally until age 2 years, when she first experienced syncope during a run. At age 3 years, she was noted to have QT prolongation on ECG screening prior to phlegmonous scar resection and since then was given a started beta-blocker (carteolol 10 mg/day). Despite beta-blocker therapy, she experienced recurrent syncope, on occasions such as running and being astonished. ECG showed QT prolongation and characteristic T wave morphology, that is, T

waves showed either broad or bifid pattern depending on heart rate (Fig. 3B-a to 3B-c). These ECG features are compatible with those of LQT2 patients.³¹ Despite atenolol (75 mg/day) therapy, at age 14 years she had repetitive syncope due to incessant TdP (Fig. 3B-d). Intravenous verapamil was effective in suppressing the TdP, and oral verapamil (120 mg/day) was started. At the same time, the beta-blocker was changed to propranolol (140 mg/day). With these medications she has remained free of syncope for more than 2 years.

R243H (*KCNQ1*) woman (Table 2; K-088)

A 52-year-old woman suffered from syncope and was noted to have QT prolongation and TdP. She had no family history of syncope and began to take propranolol (90 mg/day) and sodium channel blockers (mexiletine 400 mg/day and aprindine 60 mg/day). These medications were not successful in preventing her attacks. When aprindine was discontinued, her syncope discontinued. Because aprindine has a potent blocking action on the rapid component of the delayed rectifier potassium current I_{Kr} ,¹⁷ the drug may have aggravated her clinical features.

Functional Assay of Mutant Channels

A341V (*KCNQ1*) channel

As summarized in Table 2, we eventually found three unrelated families that carried the same heterozygous mutation: A341V (*KCNQ1*). Two of the families were associated with a heterozygous mutation in other LQTS-related genes (K-024 and K-125). Of interest, in these two families, there were three patients who were resistant to beta-blocker therapy. In contrast, although family K-001 (Table 2) had the same mutation, all members responded well to beta-blocker therapy.

To clarify the wide range of phenotypes in A341V mutants, we conducted functional analysis using a mammalian heterologous expression system. Although electrophysiologic assay of this mutation was previously performed in *Xenopus* oocytes,³² we believed it was necessary to evaluate the mutation in a mammalian expression system because oocytes have intrinsic I_{Ks} -like proteins.³³ COS7 cells transfected with WT *KCNQ1* cDNA (2 and 1 μ g/dish: Fig. 4A-a and 4A-b) displayed outward currents that slowly activated on depolarization and were typical of I_{Ks} as previously reported.^{33,34} COS7 cells transfected with A341V (*KCNQ1*) (2 μ g/dish) revealed no measurable currents (Fig. 4A-c). To simulate allelic heterozygosity, WT and A341V (*KCNQ1*) were cotransfected at an equimolar ratio (0.5 and 1 μ g/dish, respectively, Fig. 4A-d and 4A-e). One μ g WT/1 μ g mutant resulted in conductance equivalent to that of 1 μ g WT-induced current (Fig. 4A-d). Similarly, expressed current by 0.5 μ g WT/0.5 μ g A341V was half that of 1 μ g WT-induced current (Fig. 4A-e).

In multiple cells, the effect of various combinations of WT and/or mutant clones was extensively examined (Fig. 4B). In the current-voltage relations shown in Fig. 4B, each symbol indicates the mean tail current density obtained from data pool of >12 cells. At every membrane potential, cotransfected mutant A341V did not influence current density. Thus, A341V did not interfere with WT expression (no dominant negative suppression). Figure 4C shows the relationship between normalized tail currents and test potential (between –50 and +60 mV). Smooth curves are fitted to the Boltzmann equation, and there were no statistically significant changes

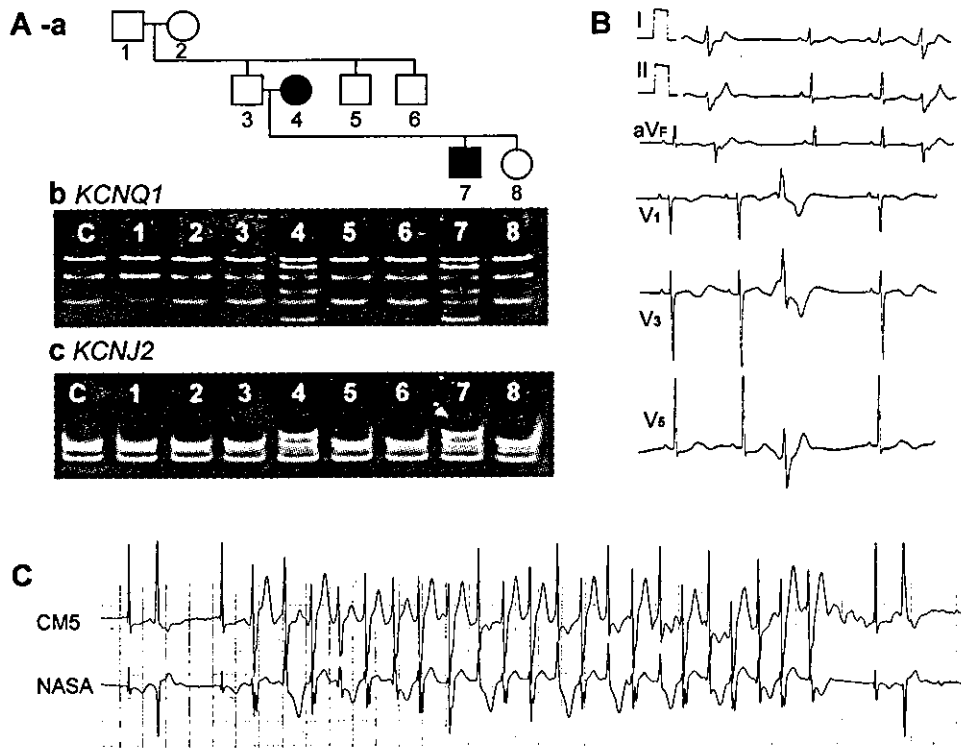


Figure 2. Identification and characterization of affected members with *KCNQ1* and *KCNJ2* mutations. A: (a) Family tree of A341V (*KCNQ1*)–G144S (*KCNJ2*) family. Consecutive numbers were given to all family members. Squares = males; circles = females; open = unaffected; closed = affected member. PCR-SSCP using the primer set for (b) *KCNQ1* and (c) *KCNJ2*: Extra bands were found only in the lanes of the 36-year-old woman (no. 4) and her son (no. 7). C indicates healthy control. B: Baseline ECG of the woman (no. 4) shown in panel A. Note QT prolongation, prominent U wave, and premature ventricular complex. C: Holter ECG recording of the son (no. 7) shown in panel A. Note bidirectional ventricular tachycardia.

in half-maximal activation potentials ($V_{1/2}$) and slope factors (V_s). Coexpression of A341V did not affect either current amplitude or voltage dependence of WT *KCNQ1* channels. Therefore, the mutant A341V subunit may not be able to coassemble with the WT subunit, thus accounting for the lack of dominant negative suppression.

S706C (KCNH2) channel

Three of the beta-blocker nonresponders were noted to have additional mutations [G144S (*KCNJ2*), S706C (*KCNH2*)]. In a different series of experiments, we conducted functional assay of the G144S (*KCNJ2*) variant using a

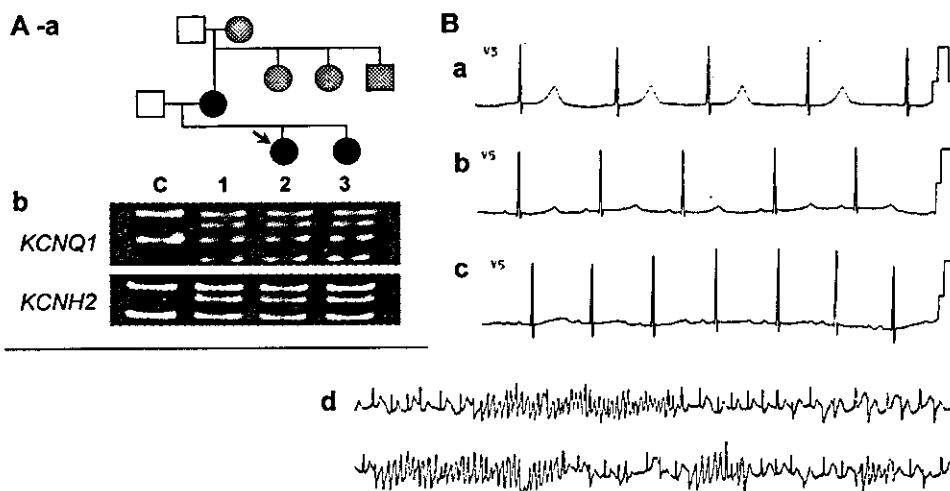


Figure 3. Identification and characterization of affected members with *KCNQ1* and *KCNH2* mutations. A: (a) Family tree of A341V (*KCNQ1*)–S706C (*KCNH2*) family. Numbers 1 through 3 are given to members available for genetic information. Squares = males; circles = females; open = asymptomatic; filled = affected and symptomatic; half-tone filled = symptomatic without available genetic information. The proband is indicated by the arrow. PCR-SSCP using the primer set for (b) *KCNQ1* and (c) *KCNH2*: Aberrant bands were noted in the lanes of the proband (no. 2), her mother (no. 1), and her younger sister (no. 3). C indicates healthy control. B: Baseline ECG of the proband no. 2 (shown in panel A). Note QT prolongation in lead V₅, (a) broad-based T wave (52 beats/min), (b) low-amplitude T wave (60 beats/min), and (c) bifid T wave (82 beats/min). (d) Electrical storm.

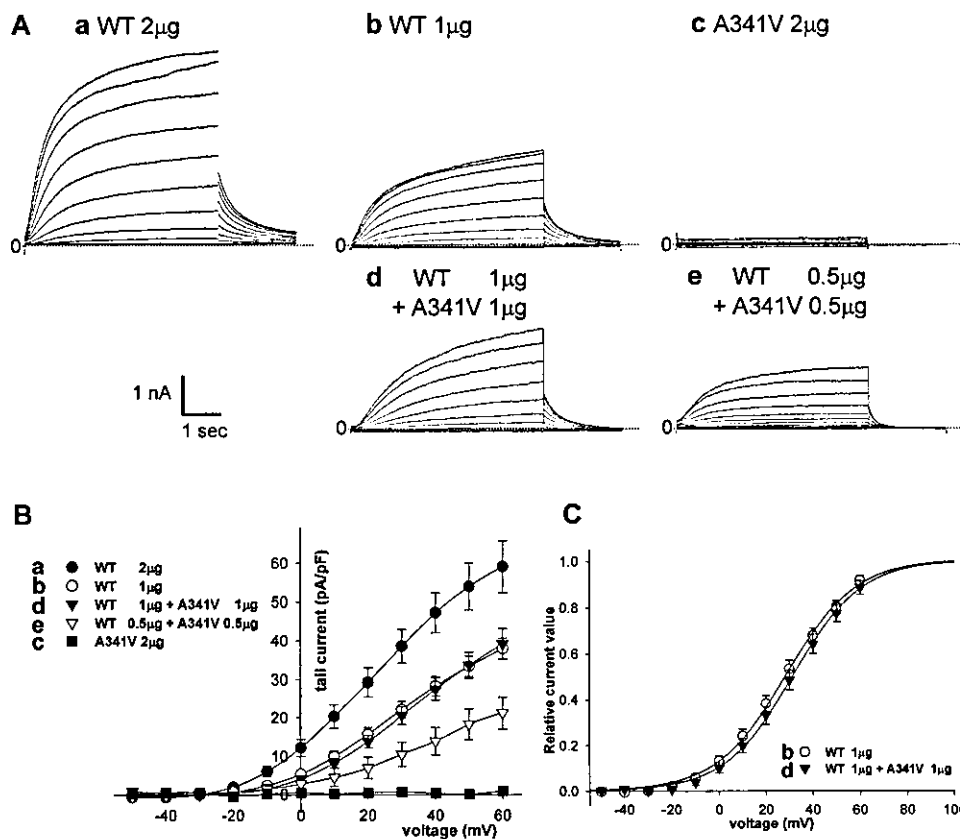


Figure 4. Macroscopic current recordings under whole-cell patch clamp of WT *KCNQ1* and/or A341V mutant expressed in COS7 cells. **A:** Representative current recordings. Holding potential was -80 mV. Depolarizing pulses (5-s duration) were applied from $+60$ to -50 mV in 10-mV decrements. Tail currents were measured on repolarization to -30 mV. Transfected cDNA volumedish is indicated above the graph. **B:** Plots of current-voltage relationships of isochronal tail current: (a) closed circles ($n = 15$), (b) open circles ($n = 15$), (c) closed triangles ($n = 15$), (d) open triangles ($n = 12$), and (e) closed squares ($n = 15$). Every measured current was normalized to cell capacitance (current density). Vertical bars indicate SEM. **C:** Normalized isochronal activation curves. For the data in the group of $1 \mu\text{g}$ WT (b; open circles) and coexpression $1 \mu\text{g}$ WT and $1 \mu\text{g}$ A341V (d; closed triangles), data points were fitted to the Boltzmann distribution. Half-maximal activation voltages were 28.31 ± 0.70 and 31.27 ± 0.58 mV, and slope factors were 14.93 ± 0.50 and 14.61 ± 0.41 , respectively.

Xenopus oocyte expression system. As reported recently by Lange et al.,³⁵ the G144S mutation was found to cause $\sim 40\%$ reduction in the inward rectifier potassium current I_{K1} ³⁶ in a heteromeric manner with the WT gene (data not shown). We then conducted a functional assay of another additive mutation [S706C (*KCNH2*)] using a mammalian heterologous expression system.

COS7 cells were transiently transfected with WT and/or mutant *KCNH2* cDNA (0.5 – $1.0 \mu\text{g}/35$ -mm dish). WT *KCNH2* current displayed rapid activation on depolarization with strong inward rectification as well as large tail currents on repolarization (Fig. 5A-a), as previously reported.⁶ S706C mutant also could display I_{Kr} , but its current density was significantly smaller than that of WT (Fig. 5A-a and 5A-c). Both S706C and WT cDNAs ($0.5 \mu\text{g}$ each) were cotransfected to mimic the heterozygous condition of the patient. In the typical traces shown in Figure 5A-b, the expressed current amplitude showed values that were intermediate between those of WT and the mutant *KCNH2* currents.

Similar experiments were conducted in multiple cells, and current densities during depolarization were measured at the end of 4-second pulse in each experiment and plotted as a function of the test potential (Fig. 5B). As depicted by representative traces in Figure 5A, the current amplitude of mutant

channels (open squares) was significantly smaller than that of WT current (closed circles). In addition, current reconstructed with mutant and WT constructs was significantly smaller (open triangles). Steady-state current densities at 10-mV depolarization were 62.15 ± 5.0 in WT, 43.13 ± 4.2 in WT/S706C*, and 27.49 ± 2.5 pA/pF in S706C*, respectively ($*P < 0.05$ vs WT). Steady-state current-potential relation showed a bell-shaped configuration and was shifted in the depolarization direction by 10 mV with cotransfection of S706C.

Channel kinetics with regard to activation and inactivation gates were examined by using the double-pulse method and tail current analyses. As summarized in Figure 5C, gating property for activation in the heterozygous (WT/S706C) condition was altered significantly toward depolarization. Fitting to the Boltzmann equation yielded $+8$ mV shift of $V_{1/2}$. In contrast, gating property for inactivation remained unchanged. Therefore, it was concluded that the S706C mutant caused a mild reduction in efficient outward I_{Kr} current, which would further prolong the action potential.

Computer Simulation of Action Potential

Nonresponders to beta-blocker in our study all were carrying heterozygous A341V *KCNQ1* mutation. Coincident

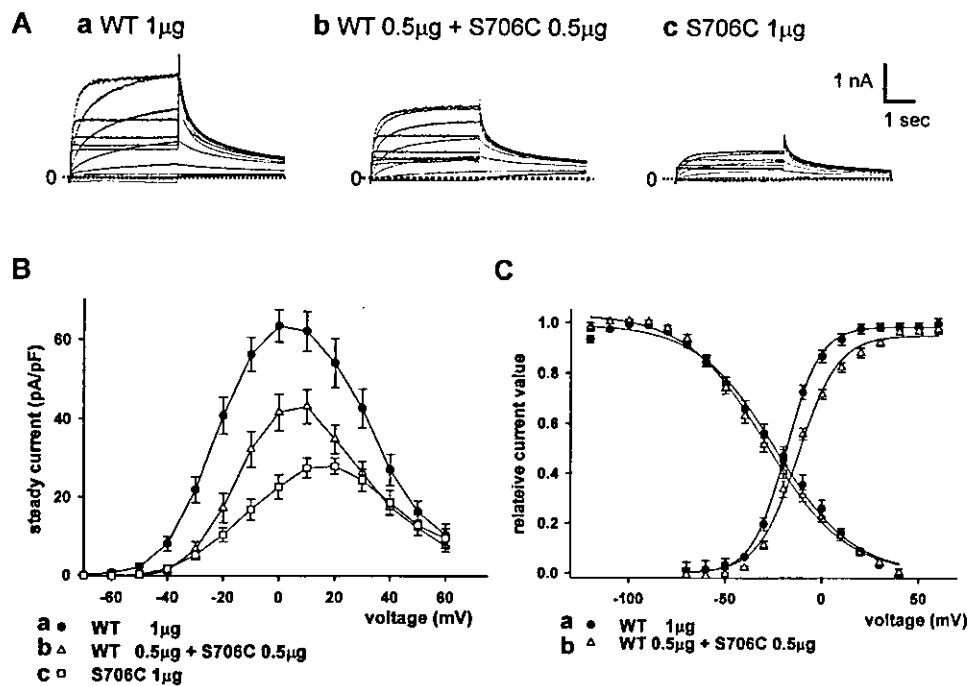


Figure 5. Macroscopic current recordings of WT and/or S706C KCNH2 channels expressed in COS7 cells. **A:** Representative current recordings. Depolarizing pulses (4-s duration) were applied from -80 mV to potentials between -70 and $+60$ mV in a 10 -mV step. Steady-state current amplitudes were measured at the end of test pulses, and tail currents after each test potential at -40 mV. Concentrations of cDNAs used for transfection (volume/dish) are indicated above each graph. **B:** Plots of steady-state current-voltage relationships: (a) WT ($1 \mu\text{g}$): closed circles ($n = 15$); (b) WT/S706C ($0.5 \mu\text{g}$ each): open triangles ($n = 13$); and (c) S706C ($1 \mu\text{g}$): open squares ($n = 18$). Measured current data were normalized to the cell capacitance (current density). Vertical bars indicate SEM. **C:** Normalized activation and inactivation curves. Activation curves were obtained by normalizing the peak tail current at -40 mV using the same protocol as in panel A. For inactivation analysis, we gave $+60$ mV depolarizing pulse (200 ms) to open the activation gate and then a preconditioning pulse (5 ms) to various potentials (between $+40$ and -120 mV in a 10 -mV step). Degree of fast inactivation was measured at the following voltage step to $+40$ mV and was normalized by the peak. For WT (a; closed circles) and WT/S706C (b; open triangles) data, the Boltzmann distribution was used to obtain $V_{1/2}$ and V_s . $V_{1/2}$ and V_s values for activation curves were -19.7 ± 0.3 and 8.7 ± 0.2 mV for WT, and $-11.4 \pm 0.9^*$ and $10.3 \pm 0.8^*$ mV for WT/S706C. Values for the inactivation curves were -24.0 ± 1.4 and -22.2 ± 1.2 mV for WT, and -26.9 ± 2.1 and -20.7 ± 0.9 mV for WT/S706C. * $P < 0.05$ vs WT.

mutations in other LQTS-related genes may account for the varied clinical features of these patients. Because it is difficult to conduct functional analyses using multiple clones in a heterologous expression system, we used the KYOTO computational model¹⁹ and examined the electrophysiologic outcome by double mutations.

The KYOTO model consists of reconstruction of APs by incorporating the majority of known sarcolemmal ion channels and transporters, sarcoplasmic reticulum, and contractile elements. Two types of AP were reconstituted by partially incorporating human experimental data into the guinea pig model: mid-myocardial (M) and epicardial (Epi) cells as described in the Methods section (Fig. 6A). In each type of cell, we simulated how second mutations modified arrhythmogenesis in the reconstituted LQT1 model induced by A341V mutation. To mimic more completely the condition found in our beta-blocker nonresponders, we introduced experimental data into ion channels that were found to be affected: (1) 50% reduction in I_{Ks} for the LQT1 model—A341V (*KCNQ1*); (2) $V_{1/2}$ of I_{Kr} activation shift by 8 mV in the depolarization direction for the LQT2 model—S706C (*KCNH2*); and (3) 40% reduction in I_{K1} amplitude for LQT7 model—G144S (*KCNJ2*) (adopted from reference 35).

In the LQT1 model (Fig. 6B), half-reduction in I_{Ks} produced almost equivalent prolongation of action potential duration (APD) in M and Epi cells (solid lines); therefore, the transmural dispersion of repolarization (TDR; differences

APD between M and Epi) represented a small decrease (66 ms in normal and 64 ms LQT1). I_{Kr} or I_{K1} modulation measured experimentally as described earlier was incorporated into the LQT1 model to simulate the double heterozygosity in our patients (LQT1+2 in K-125 and LQT1+7 in K-024) (Fig. 6C and 6D). Additional alterations caused further prolongation of APD and mild TDR increases (72 ms in LQT1+2 and 74 ms in LQT1+7 model).

In M cell of the LQT1+7 model, APD at 90% repolarization from the overshoot (APD₉₀) lengthened more prominently (5.1% in LQT1+2, 12.5% in LQT1+7, each increase from LQT1) than APD₅₀ (5.9% and 9.2%, respectively), probably because I_{K1} affects the final phase of repolarization. Similarly, including I_{K1} modulation slowed the repolarization rate (dV/dt) at APD₉₀ more significantly than at APD₅₀: 0.46, 0.38, and 0.30 mV/ms at APD₅₀ and 2.49, 2.37, and 1.32 mV/ms at APD₉₀ in LQT1, LQT1+2, and LQT1+7, respectively. The reduction in I_{K1} depolarized the resting membrane potential from -92.7 to -90.7 mV. The results induced by the I_{K1} suppression model are consistent with previous observations in an animal model, even with suppression of I_{K1} alone.³⁷

Lowering extracellular K^+ from 4.0 to 3.0 mEq/L produced APD prolongation (dotted lines in Fig. 7B to 7D), especially in M cells, which yielded TDR increase in LQT1 (72 ms) and drastically changed those in double-altered models (110 ms in LQT1+2 and 118 ms in LQT1+7).

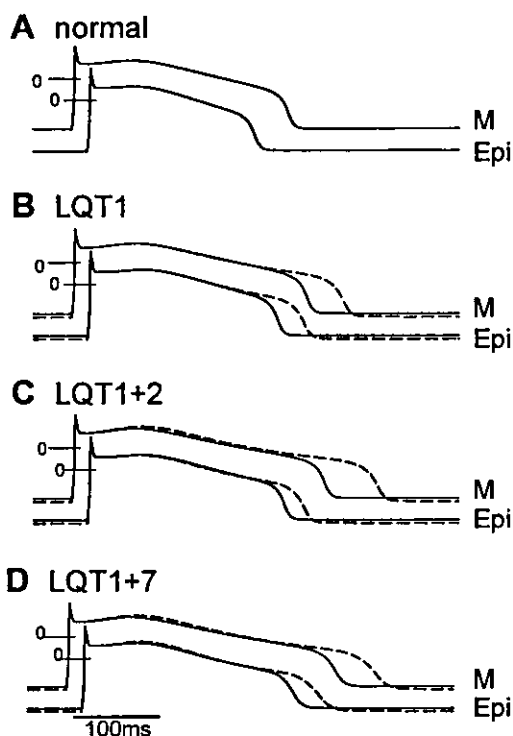


Figure 6. Action potential simulation study in the combined LQTS model. Two types of action potential (AP) models at cycle length of 1,000 ms: M = mid-myocardial cell model; epi = epicardial cell model. Solid lines show AP configurations in normal extracellular K^+ concentration (4 mEq/L), dashed lines in low K^+ concentration (3 mEq/L). A: Normal type model; B: LQT1 model obtained by 50% I_{Ks} reduction; C: LQT1+2 model obtained by 50% reduction of I_{Ks} with a +8 mV shift of activation curve for I_{Ks} ; D: LQT1+7 model obtained by 50% reduction of I_{Ks} and 40% reduction of I_{K1} .

Shimizu and Antzelevitch³⁸ elegantly proved that to induce TdP in their LQT1 model of arterially perfused wedge preparations of canine left ventricle, not only I_{Ks} reduction but also beta-adrenergic stimulation was required. The findings were compatible with the clinical features of LQT1 patients. In a final series of experiments, we altered major ion currents by mimicking beta-adrenergic stimulation as described in the Methods section. In the presence of beta-adrenergic stimulation in the LQT1 model, TDR dramatically increased (>100 ms in every beats), and an early afterdepolarization (EAD) occurred (the fifth beat of M cell series, solid line, Fig. 7A). EAD would trigger TdP in the clinical setting.

In the LQT1+2 model (Fig. 7B), upon beta-adrenergic stimulation, an additive effect of I_{Ks} modulation produced a more profound increase in TDR and frequent EADs in M cell (solid line) than in the LQT1 model. In the LQT1+7 model (Fig. 7C), upon beta-adrenergic stimulation, I_{K1} suppression also caused an increase in TDR and the occurrence of EADs in M cell. Transient depolarizations such as small delayed afterdepolarization (DADs) were observed in the diastolic phase of M cell in the LQT1+7 series (Fig. 7C, solid line), as previously reported.³⁹ Thus, based upon the KYOTO computational model, it was postulated that these genetic modifiers in addition to the A341V (*KCNQ1*) mutation increase the arrhythmogenic risk in our patients.

Discussion

Heterogeneity of Clinical Phenotype and Beta-Blocker Response

Recent advances in studies of hereditary arrhythmia allowed us to conduct gene-specific treatment. Beta-adrenoceptor blockers have become first-line therapy with high efficacy in LQT1 patients,^{10,12,13} and Shimizu and Antzelevitch^{11,38} showed the cellular mechanism in arterially perfused wedge preparations. On the other hand, some LQT1 cases were refractory to this therapy, and the reasons remain unknown.^{10,13} In the present study, 18 LQT1 patients in whom 6 different *KCNQ1* variants were identified were examined in this regard. There were 4 nonresponders to the therapy (22%). This percentage in the 70-month observation period was comparable to the ~20% previously reported.^{10,13} One of the patients took aprindine, which modulated the efficacy of beta-blocker treatment. The other 3 patients from 2 families all were carriers of the mutation heterozygous A341V (*KCNQ1*). We then conducted extensive genetic analyses in 18 patients from 12 families and found that these 2 families had two heterozygous mutations in other LQTS-related genes: G144S (*KCNJ2*) and S706C (*KCNH2*). In contrast, we failed to identify any additional mutations in LQTS-related genes in the remaining 10 families.

Alanine at codon 341 is a hot-spot *KCNQ1* mutation, and a number of LQT1 families carrying this variant have been reported with their clinical features.^{1,29,32,40-42} There were 8 symptomatic and heterozygous A341V carriers among our study patients. Three of these patients who had A341V alone

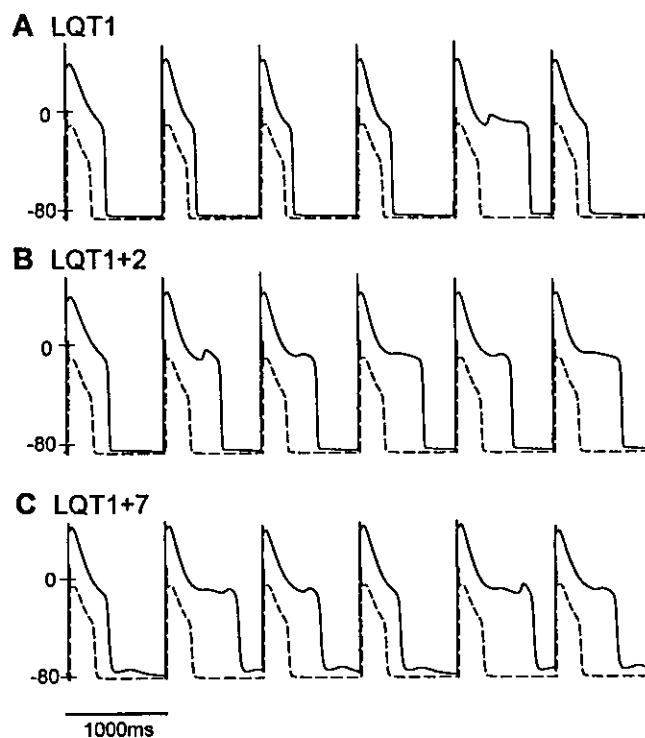


Figure 7. Action potential simulation study in beta-adrenergic stimulation. Three types of action potentials (AP) in LQT1 (A), LQT1+2 (B), and LQT1+7 (C) models under beta-adrenergic stimulation. Solid lines indicate AP trains in the mid-myocardial (M) model, dashed lines in the isochronal epicardial (Epi; reduced current amplitude) model.

(K-001) were good responders to beta-blocker therapy. In contrast, among 5 members with double mutations (K-024 and K-125), 3 were nonresponders. As we confirmed with the functional outcome of A341V mutation by electrophysiologic techniques (Fig. 4), this variant produced a 50% current reduction in the heterozygous condition and exerted no dominant negative effect. Both results partially explained the phenotype of patients with A341V alone. In other words, additional mutations in either *KCNJ2* or *KCNH2* appeared to modify the clinical aspects.

Simulation Study and Implications for Clinical Features

How can we learn the phenotype modified by these double mutations? Transgenic mice or gene transfer techniques using virus vector^{43,44} have helped us to understand much about the mechanism of LQTS, but it is difficult in the presence of multiple mutations. Therefore, we conducted a computer AP simulation by adopting the KYOTO model¹⁹ and by including some human experimental data. Cellular electrophysiologic characteristics were examined extensively (Figs. 6 and 7) by incorporating multiple current dysfunctions measured in the heterologous expression system (Fig. 4 and 5).

Beta-adrenergic stimulation in the LQT1 model induced a larger TDR and increased risk for EADs, as demonstrated by Shimizu and Antzelevitch³⁸ in wedge preparations and as seen in clinical settings. Additional reduction in either I_{K1} or I_{Kr} produced marked electrical instability, especially in the presence of low K^+ or beta-adrenergic stimulation. Thus, additional genetic alterations may be one cause for the severe phenotype in LQTS.

To our knowledge, there has been only one case report of double mutations of LQTS-related genes (*KCNQ1* and *KCNH2*).⁴⁵ Two members of the affected family (LQT1+2) were severely symptomatic and resistant to beta-blocker therapy. Hypokalemia due to diarrhea and vomiting appeared to be an aggravating factor in these cases. Because, based on our computer model, hypokalemia is a definite risk factor in the case of LQT1+2 model (Fig. 6C), K supplement therapy would have been effective in their cases.

Study Limitations

Our clinical data were obtained in a relatively small number of Japanese LQTS families; therefore, the extent to which the data can be applied more generally must be verified in a larger cohort. We conducted computer AP simulation studies using the KYOTO model, which consists of reconstruction of guinea pig APs. Although we replaced some major elements with human experimentally outcome (Table 1), we must await more detailed information on human cardiac myocyte electrophysiology in both normal and genetically altered conditions. Further study is required to develop a multicellular model with predictable ECG as well as a whole heart computer model.

Conclusion

We provide evidence that multiple mutations in different LQTS-related genes may influence phenotype severity and reduce beta-blocker effectiveness in LQT1 patients. Previous reports showed that approximately 20% of LQT1 patients are resistant to beta-blocker therapy.^{10,13} We suggest that there may be additional mutations in such patients, and that it is

of critical importance to conduct a complete genetic survey of all LQTS-related genes, even if one possible mutation has already been identified.

Acknowledgments: The authors thank all the family members for participating in this study; Dr. J. Barhanin for *KCNQ1* and *KCNE1* cDNA clones; Dr. M.C. Sanguinetti for *KCNH2* cDNA; Dr. C. Vandenberg for the human *KCNJ2* cDNA; Dr. J. Tytgat for the pGEMHE oocyte expression vector; and Ms. K. Tsuji and Mr. Fukao for expert technical assistance.

References

1. Wang Q, Curran ME, Splawski I, Burn TC, Millholland JM, VanRaay TJ, Shen J, Timothy KW, Vincent GM, de Jager T, Schwartz PJ, Towbin JA, Moss AJ, Atkinson DL, Landes GM, Connors TD, Keating MT: Positional cloning of a novel potassium channel gene: KVLQT1 mutations cause cardiac arrhythmias. *Nat Genet* 1996;12:17-23.
2. Curran ME, Splawski I, Timothy KW, Vincent GM, Green ED, Keating MT: A molecular basis for arrhythmia: HERG mutations cause long QT syndrome. *Cell* 1995;80:795-803.
3. Wang Q, Shen J, Splawski I, Atkinson D, Li Z, Robinson JL, Moss AJ, Towbin JA, Keating MT: SCN5A mutations associated with an inherited cardiac arrhythmia, long QT syndrome. *Cell* 1995;80:805-811.
4. Mohler PJ, Schott JJ, Gramolini A, Dilly KW, Guatimosim S, Dubell WH, Song LS, Haurongné K, Kyndt F, Ali ME, Rogers TB, Lederer WJ, Escande D, Marec HL, Bennett V: Ankyrin-B mutation causes type 4 long-QT cardiac arrhythmia and sudden cardiac death. *Nature* 2003;421:634-639.
5. Splawski I, Tristani-Firouzi M, Lehmann MH, Sanguinetti MC, Keating MT: Mutations in the hminK gene cause long QT syndrome and suppress I_{Ks} function. *Nat Genet* 1997;17:338-340.
6. Abbott GW, Sesti F, Splawski I, Buck ME, Lehmann MH, Timothy KW, Keating MT, Goldstein SA: MiRP1 forms I_{Kr} potassium channels with HERG and is associated with cardiac arrhythmia. *Cell* 1999;97:175-187.
7. Tawil R, Ptacek LJ, Pavlakis SG, DeVivo DC, Penn AS, Ozdemir C, Griggs RC: Andersen's syndrome: Potassium-sensitive periodic paralysis, ventricular ectopy, and dysmorphic features. *Ann Neurol* 1994;35:326-330.
8. Plaster NM, Tawil R, Tristani-Firouzi M, Canún S, Bendahhou S, Tsunoda A, Donaldson MR, Iannaccone ST, Brunt E, Barohn R, Clark J, Deymeer F, George AL Jr, Fish FA, Hahn A, Nitu A, Ozdemir C, Serdaroglu P, Subramony SH, Wolfe G, Fu YH, Ptacek LJ: Mutations in Kir2.1 cause the developmental and episodic electrical phenotypes of Andersen's syndrome. *Cell* 2001;105:511-519.
9. Ai T, Fujiwara Y, Tsuji K, Otani H, Nakano S, Kubo Y, Horie M: Novel *KCNJ2* mutation in familial periodic paralysis with ventricular dysrhythmia. *Circulation* 2002;105:2592-2594.
10. Schwartz PJ, Priori SG, Spazzolini C, Moss AJ, Vincent GM, Napolitano C, Denjoy I, Guicheney P, Breithardt G, Keating MT, Towbin JA, Beggs AH, Brink P, Wilde AAM, Toivonen L, Zareba W, Robinson JL, Timothy KW, Corfield V, Watanasirichaigoon D, Corbett C, Haverkamp W, Schulze-Bahr E, Lehmann MH, Schwartz K, Coumel P, Bloise R: Genotype-phenotype correlation in the long-QT syndrome: gene-specific triggers for life-threatening arrhythmias. *Circulation* 2001;103:89-95.
11. Shimizu W, Antzelevitch C: Differential effects of beta-adrenergic agonists and antagonists in LQT1, LQT2 and LQT3 models of the long QT syndrome. *J Am Coll Cardiol* 2000;35:778-786.
12. Schwartz PJ, Priori SG, Napolitano C: The long QT syndrome. In Zipes DP, Jalife J, eds: *Cardiac Electrophysiology: From Cell to Bedside*. Third Edition. Philadelphia:WB Saunders, 2000:597-615.
13. Moss AJ, Zareba W, Hall WJ, Schwartz PJ, Crampton RS, Benhorin J, Vincent M, Locati EH, Priori SG, Napolitano C, Medina A, Zhang L, Robinson JL, Timothy K, Towbin JA, Andrews ML: Effectiveness and limitations of β -blocker therapy in congenital Long-QT syndrome. *Circulation* 2000;101:616-623.
14. Moss AJ, Robinson J: Clinical features of the idiopathic long QT syndrome. *Circulation* 1992;85(Suppl I):I-140-I-144.
15. Bazett H: An analysis of the time relations of electrocardiograms. *Heart* 1920;7:353-367.
16. Kunkel LM, Smith KD, Boyer SH, Bargaonkar DS, Wachtel SS, Miller OJ, Breg WR, Jones HW Jr, Rary JM: Analysis of human Y-chromosome specific reiterated DNA in chromosome variants. *Proc Natl Acad Sci USA* 1977;74:1245-1249.

17. Yoshida H, Horie M, Otani H, Takano M, Tsuji K, Kubota T, Fukunami M, Sasayama S: Characterization of a novel missense mutation in the pore of HERG in a patient with long QT syndrome. *J Cardiovasc Electrophysiol* 1999;10:1262-1270.
18. Kubota T, Shimizu W, Kamakura S, Horie M: Hypokalemia-induced long QT syndrome with an underlying novel missense mutation in S4-S5 linker of KCNQ1. *J Cardiovasc Electrophysiol* 2000;11:1048-1054.
19. Matsuoka S, Sarai N, Kuratomi S, Ono K, Noma A: Role of individual ionic current systems in ventricular cells hypothesized by a model study. *Jpn J Physiol* 2003;53:105-123.
20. Cohen NM, Lederer WJ: Calcium current in single human cardiac myocytes. *J Cardiovasc Electrophysiol* 1993;4:422-437.
21. Li GR, Feng J, Yue L, Carrier M, Nattel S: Evidence for two components of delayed rectifier K⁺ current in human ventricular myocytes. *Circ Res* 1996;78:689-696.
22. Péréon Y, Demolombe S, Baró I, Drouin E, Charpentier F, Escande D: Differential expression of KvLQT1 isoforms across the human ventricular wall. *Am J Physiol* 2000;278:H1908-H1915.
23. Näbauer M, Beuckelmann DJ, Erdmann E: Characteristics of transient outward current in human ventricular myocytes from patients with terminal heart failure. *Circ Res* 1993;73:386-394.
24. Li GR, Feng J, Yue L, Carrier M: Transmural heterogeneity of action potentials and I_{to1} in myocytes isolated from the human right ventricle. *Am J Physiol* 1998;275:H369-H377.
25. Näbauer M, Beuckelmann DJ, Überfuhr P, Steinbeck G: Regional differences in current density and rate-dependent properties of the transient outward current in subepicardial and subendocardial myocytes of human left ventricle. *Circulation* 1996;93:168-177.
26. Koumi S, Backer CL, Arentzen CE: Characterization of inwardly rectifying K⁺ channel in human cardiac myocytes: Alterations in channel behavior in myocytes isolated from patients with idiopathic dilated cardiomyopathy. *Circulation* 1995;92:164-174.
27. Maltsev VA, Sabbah HN, Higgins RS, Silverman N, Lesch M, Undrovinas AI: Novel, ultraslow inactivating sodium current in human ventricular cardiomyocytes. *Circulation* 1998;98:2545-2552.
28. Zeng J, Rudy Y: Early afterdepolarizations in cardiac myocytes: mechanism and rate dependence. *Biophys J* 1995;68:949-964.
29. Li H, Chen Q, Moss AJ, Robinson J, Goytia V, Perry JC, Vincent M, Priori SG, Lehmann MH, Denfield SW, Duff D, Kaine S, Shimizu W, Schwartz PJ, Wang Q, Towbin JA: New mutations in the KVLQT1 potassium channel that cause long-QT syndrome. *Circulation* 1998;97:1264-1269.
30. Kubota T, Horie M, Takano M, Yoshida H, Takenaka K, Watanabe E, Tsuchiya T, Otani H, Sasayama S: Evidence for a single nucleotide polymorphism in the KCNQ1 potassium channel that underlies susceptibility to life-threatening arrhythmias. *J Cardiovasc Electrophysiol* 2001;12:1223-1229.
31. Takenaka K, Ai T, Shimizu W, Kobori A, Ninomiya T, Otani H, Kubota T, Takaki H, Kamakura S, Horie M: Exercise stress test amplifies genotype-phenotype correlation in the LQT1 and LQT2 forms of the long-QT syndrome. *Circulation* 2003;107:838-844.
32. Wang Z, Tristani-Firouzi M, Xu Q, Lin M, Keating MT, Sanguinetti MC: Functional effects of mutations in KvLQT1 that cause long QT syndrome. *J Cardiovasc Electrophysiol* 1999;10:817-826.
33. Sanguinetti MC, Curran ME, Zou A, Shen J, Spector PS, Atkinson DL, Keating MT: Coassembly of KvLQT1 and minK (IsK) proteins to form cardiac I_{Ks} potassium channel. *Nature* 1996;384:80-83.
34. Barhanin J, Lesage F, Guillemare E, Fink M, Lazdunski M, Romey G: KvLQT1 and IsK (minK) proteins associate to form the I_{Ks} cardiac potassium current. *Nature* 1996;384:78-80.
35. Lange PS, Er F, Gassanov N, Hoppe UC: Andersen mutations of KCNJ2 suppress the native inward rectifier current I_{K1} in a dominant-negative fashion. *Cardiovasc Res* 2003;59:321-327.
36. Kubo Y, Baldwin TJ, Jan YN, Jan LY: Primary structure and functional expression of a mouse inward rectifier potassium channel. *Nature* 1993;362:127-133.
37. Miake J, Marbán E, Nuss HB: Functional role of inward rectifier current in heart probed by Kir2.1 overexpression and dominant-negative suppression. *J Clin Invest* 2003;111:1529.
38. Shimizu W, Antzelevitch C: Cellular basis for the ECG features of the LQT1 form of the long-QT syndrome: Effects of beta-adrenergic agonists and antagonists and sodium channel blockers on transmural dispersion of repolarization and torsade de pointes. *Circulation* 1998;98:2314-2322.
39. Tristani-Firouzi M, Jensen JL, Donaldson MR, Sansone V, Meola G, Hahn A, Bendahhou S, Kwiecinski H, Fidzianska A, Plaster N, Fu YH, Ptacek LJ, Tawil R: Functional and clinical characterization of KCNJ2 mutations associated with LQT7 (Andersen syndrome). *J Clin Invest* 2002;110:381-388.
40. Splawski I, Shen J, Timothy KW, Lehmann MH, Priori S, Robinson JL, Moss AJ, Schwartz PJ, Towbin JA, Vincent GM, Keating MT: Spectrum of mutations in long-QT syndrome genes. KVLQT1, HERG, SCN5A, KCNE1, and KCNE2. *Circulation* 2000;102:1178-1185.
41. Russell MW, Dick M, Collins FS, Brody LC: KVLQT1 mutations in three families with familial or sporadic long QT syndrome. *Hum Mol Genet* 1996;5:1319-1324.
42. de Jager T, Corbett CH, Badenhorst JC, Brink PA, Corfield VA: Evidence of a long QT founder gene with varying phenotypic expression in South African families. *J Med Genet* 1996;33:567-573.
43. Demolombe S, Lande G, Charpentier F, van Roon MA, van den Hoff MJ, Toumaniantz G, Baro I, Guihard G, LeBerre N, Corbier A, de Bakker J, Opthof T, Wilde A, Moorman AF, Escande D: Transgenic mice overexpressing human KvLQT1 dominant-negative isoform. Part I: Phenotypic characterisation. *Cardiovasc Res* 2001;50:314-327.
44. Li RA, Miake J, Hoppe UC, Johnes DC, Marbán E, Nuss HB: Functional consequences of the arrhythmogenic G306R KvLQT1 K⁺ channel mutant probed by viral gene transfer in cardiomyocytes. *J Physiol* 2001;533.1:127-133.
45. Berthet M, Denjoy I, Donger C, Demay L, Hammoude H, Klug D, Schulze-Bahr E, Richard P, Funke H, Schwartz K, Coumel P, Hainque B, Guicheney P: C-terminal HERG mutations: The role of hypokalemia and a KCNQ1-associated mutation in cardiac event occurrence. *Circulation* 1999;99:1464-1470.

Reconstruction of action potential of repolarization in patients with congenital long-QT syndrome

Akihiko Kandori¹, Wataru Shimizu², Miki Yokokawa²,
Shiro Kamakura², Kunio Miyatake², Masahiro Murakami³,
Tsuyoshi Miyashita¹, Kuniomi Ogata¹ and Keiji Tsukada⁴

¹ Central Research Laboratory, Hitachi, Ltd, 1-280 Higashi-koigakubo, Kokubunji, Tokyo 185-8601, Japan

² National Cardiovascular Center, Osaka, Japan

³ Hitachi High-technologies, Ibaraki, Japan

⁴ Okayama University, Okayama, Japan

E-mail: kandori@rd.hitachi.co.jp

Received 19 January 2004

Published 4 May 2004

Online at stacks.iop.org/PMB/49/2103

DOI: 10.1088/0031-9155/49/10/019

Abstract

A method for reconstructing an action potential during the repolarization period was developed. This method uses a current distribution—plotted as a current-arrow map (CAM)—calculated using magnetocardiogram (MCG) signals. The current arrows are summarized during the QRS complex period and subtracted during the ST-T wave period in order to reconstruct the action-potential waveform. To ensure the similarity between a real action potential and the reconstructed action potential using CAM, a monophasic action potential (MAP) and an MCG of the same patient with type-I long-QT syndrome were measured. Although the MAP had one notch that was associated with early afterdepolarization (EAD), the reconstructed action potential had two large and small notches. The small notch timing agreed with the occurrence of the EAD in the MAP. On the other hand, the initiation time of an abnormal current distribution coincides with the appearance timing of the first large notch, and its end time coincides with that of the second small notch. These results suggest that a simple reconstruction method using a CAM based on MCG data can provide a similar action-potential waveform to a MAP waveform without having to introduce a catheter.

(Some figures in this article are in colour only in the electronic version)

1. Introduction

The action potential is a basic unit of electrical activation in the heart. It has a variety of waveforms depending on the atrial myocardium, the ventricular myocardium and the conduction pathways (AV node, His, bundle branches and Purkinje) (Hoffman and Cranefield 1960). To detect the action potential, monophasic action potential (MAP) recording has been used since the first comparison study between action potential and MAP was performed (Hoffman *et al* 1959). MAP recordings revealed afterdepolarizations during the late repolarization period in two patients with congenital long-QT syndrome (Gavrilescu and Luca 1978). Furthermore, an early afterdepolarization (EAD) was detected on a MAP of patients with idiopathic long-QT syndrome (Bonatti *et al* 1983). It has also been reported that the appearance of the EAD in the LQT group was associated with an increased amplitude of the late component of the TU complex and that the corrected QT (QTc) interval was prolonged by isoproterenol (Shimizu *et al* 1991). Moreover, it has been reported that the EAD triggered the ventricular premature complex (Shimizu *et al* 1994, 1995) and *torsades de pointes* in patients with long-QT syndrome (Kurita *et al* 1997, Vos *et al* 2000).

Electrical propagation of the ventricular action potential was studied using a one-dimensional Beeler-Reuter cable model (Beeler and Reuter 1977). The model has been used to reconstruct two-dimensional electrical propagation (Roberge *et al* 1986, Delgado *et al* 1990). These studies suggested that threshold requirements for active propagation were lower for transverse propagation than for longitudinal propagation, which is associated with a line of gap junctions. Although the model still has some problems (fibre orientation, three-dimensional complexity, etc, in the real heart), it is very useful for understanding the mechanism of electrical activation in the myocardial muscle.

The repolarization wave represents current flow which is originated from the potential difference of action potential mainly between endocardial and epicardial regions. Thus, a magnetocardiogram (MCG) can depict the potential derivative at each time point, i.e. the difference of action potential of two regions. The MCG has a high spatial resolution for cardiac electrical sources because it suffers little interference from various organs such as the bones and the lungs (Hosaka *et al* 1976, Cuffin 1978). Electrical distributions have been analysed mathematically by a multiple-source model (Karp *et al* 1980) and a realistic torso model (Nenonen *et al* 1991). To simplify the analysis, we have used a tangential vector calculated from the normal component of a magnetic field, because it reflects an electrically activated current distribution (Hosaka and Cohen 1976, Tsukada *et al* 1998, 1999, Miyashita *et al* 1998, Horigome *et al* 1999, Kandori *et al* 2001a, 2001b, 2002, Kanzaki *et al* 2003). In the visualization of a tangential vector, MCGs of adult patients with long-QT syndrome (LQTS) had an abnormal current distribution in the cases of LQT1 and LQT2 types (Kandori *et al* 2002).

In the present study, we developed a method that uses MCG signals to reconstruct an action potential in a repolarization phase. We then verified that this method can be used to estimate the presence of the EAD in LQTS patients.

2. Methods

2.1. Relationship between action potential and electrocardiogram

The relationship between a cell-membrane ionic current, an action potential in ventricular muscle and an electrocardiogram can be represented by figure 1. When the selectivity of the ions in the current increases, an ionic current occurs in accordance with the ionic potential